酵母でディスプレーシステム開発

酵母は真核細胞であるため、細菌での発現が難しいと考えられるたんぱく質のディスプレーにも適用できると期待される。酵母の細胞表層は、多糖であるグルカン層と、それに結合して細胞表層に局在する糖たんぱく質とからなる頑丈な細胞壁で覆われている。酵母から動植物の広い範囲にわたって真核生物の細胞表層に局在する糖たんぱく質（細胞表層たんぱく質）は、N-末端に分泌シグナルとC-末端にGPI（グリコシル・フォスファチジル・イノシトール）アンカー付着シグナルという2つのシグナルをもち、GPIアンカーを介してグルカン層に共有結合する。

酵母Saccharomyces cerevisiaeにおける各種細胞表層ディスプレー系では、細胞表層たんぱく質であるα-アグルチニン（性凝集素たんぱく質）やα-アグルチニンのGPIアンカーによる表層への結合を利用するシステムが開発されている（Fig 2 a、b）。現在までに酵母では、ペプチドから分子量のかなり大きなたんぱく質（例えば分子量136kDaのAspergillus aculeatus β-glucosidase）まで多種多様な分子が、ディスプレーされている。また細胞1つ当たりでは、10^5〜10^6個とかなり多くの分子をディスプレーできることが明らかとなっている。

さらに私たちの研究グループは、Flo1たんぱく質（凝集性酵母におけるレクチン様凝集たんぱく質であるフロッキュリン）のN-末側の細胞付着領域を活用した、新しい発想の細胞表層ディスプレー系を、神戸大学発のベンチャー企業、バイオ・エナジー（兵庫県尼崎市）と共同で開発することに成功した（Fig 2 c）。

Flo1は全長1356アミノ酸残基からなるたんぱく質（伸びた構造をもち、全長300nm程度）であり、N-末端より1087残基までが凝集機能ドメイン（酵母表層グルカン層と相互作用するレクチン様たんぱく質）、1087-1356までが細胞壁アンカー領域と考えられている。新しい系は、Flo1のN-末端側の1099アミノ酸残基を用い、そのC-末端側にディスプレーしたい目的たんぱく質を融合する系である。

発現されたたんぱく質は、Flo1の凝集機能ドメインによって酵母細胞表層のグルカン層に付着固定化される。すなわち、細胞表層に付着するたんぱく質機能を利用した細胞表層ディスプレー系であり、愛称で“ひっつき虫”型と呼ばれている。このシステムでは、目的たんぱく質のN-末端を融合させることになるが、リパーゼのようにC-末端側に活性サイトのあるものを活性な形で細胞表層ディスプレーするには極めて優れた系である。このように、酵母では各種のディスプレー系が利用可能になりつつある。

バイオマスからエタノールを直接生産

アミラーゼやセルラーゼを細胞表層工学の手法でディスプレーした新機能酵母（アーミング酵母）を創製すれば、でん粉やセルロースといったバイオマスから直接バイオエタノールを生産できると考えられる。すなわち、細胞表層に集積されたアミラーゼやセルラーゼによりでん粉やセルロースはグルコースまで分解され、直ちに酵母に取り込まれて酵母が本来もつ代謝系

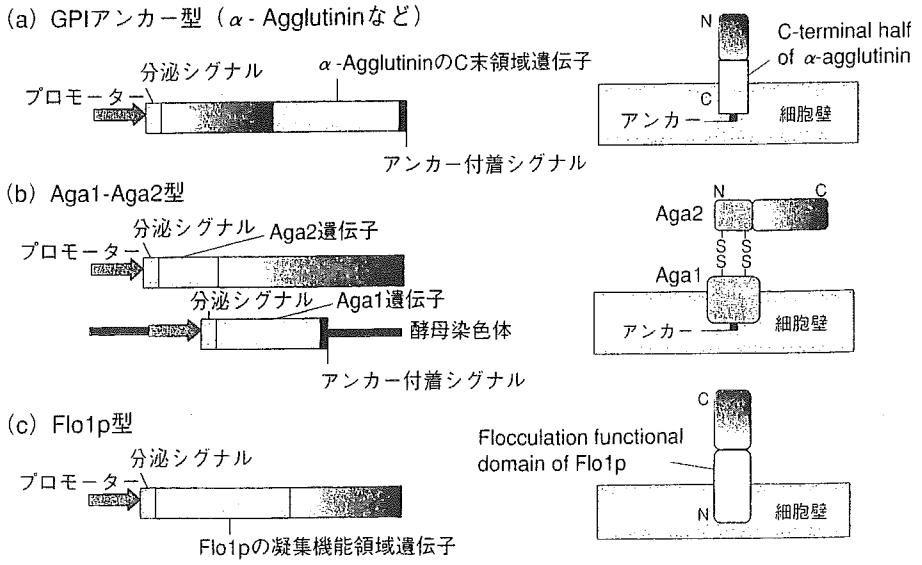

Fig 2　酵母を利用する細胞表層ディスプレーシステムの事例

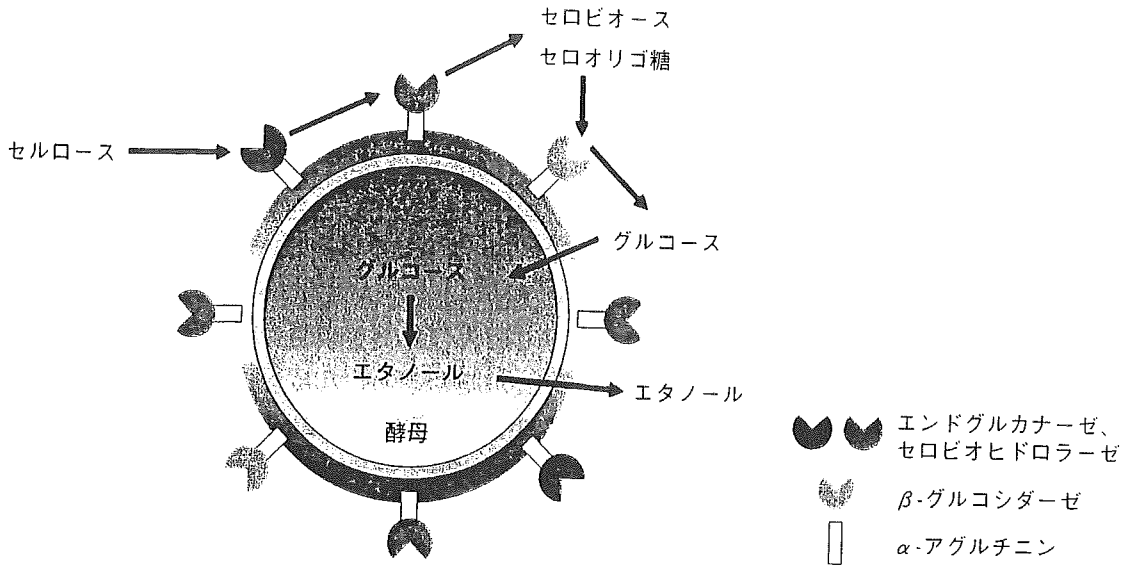

Fig 3　アーミング酵母を用いたセルロースからのエタノール直接生産

によりエタノールに変換される。ここでは、セルロースからの直接エタノール発酵が可能なアーミング酵母の創製について紹介する（Fig 3）。

セルロースは結晶領域と非結晶領域が混在する強い繊維であり、その分解には複数の酵素の関与が必要である。まずエンド型セルラーゼであるエンドグルカナーゼが非結晶領域を分解し、生じた末端からエキソ型セルラーゼであるエキソセロビオヒドロラーゼが結晶領域を分解する。さらに両セルラーゼの相乗作用で、セルロースはセロビオースを主生成物とする可溶性のセロオリゴ糖にまで分解された後、β-グルコシダーゼによってグルコースへと変換される。

従ってFig 3に示すように、各種セルロース資源から直接バイオエタノール生産できる酵母を創製するには、これらのセルラーゼを細胞表層に同時にディスプレーして集積する必要がある。私たちは、これら3種類の酵素を、α-アグルチニンを用いて同時にディスプレーすることを試みた。各酵素の細胞表層への活性な形でのディスプレーが確認できたため、セルロースを唯一の炭素源として発酵実験を行ったところ、理論収率の90%以上と効率よくバイオエタノールを生産できることを確かめた。これは、酵母によるセルロース原料からの直接エタノール発酵としては世界初の成果例である。また、細胞表層に複数の酵素を集積して協同的に作用できることを示せた点でも、大きな一歩であろう。

乳酸菌や大腸菌での応用も活発に

これまでに述べた酵母における細胞表層ディスプレー系に加えて、グラム陰性およびグラム陽性の各種細菌を利用した各種の表層ディスプレー系が開発されている。中でもグラム陽性細菌であるLactobacillusやLactococcus属に代表される乳酸菌を利用した細胞表層ディスプレー系の研究は進んでいる。

乳酸菌は人の健康にも有効な菌群であり、古来より食品製造や有用物質生産に幅広く利用されてきた。乳酸菌の細胞表層ディスプレー系を開発し、経口ワクチンなどに応用しようとする試みは特に活発である。これは、乳酸菌の細胞表層のペプチドグリカン層に天然の免疫増進（アジュバント）効果があり、抗原を表層ディスプレーした乳酸菌が非常に魅力的なワクチンになると期待されるためである。

多くの場合、グラム陽性菌の表層たんぱく質の細胞表層へのソーティングが共通のLPXTGモチーフ（約30のアミノ酸残基からなる疎水性コアと、正電荷のあるアルギニンまたはリジンの末端部からなる）によって行われていることを利用し、細胞表層ディスプレー系が開発されている。

一方、グラム陰性菌としては、主として大腸菌Esherichia coliが用いられ、多くの応用例が報告されている。例えば外膜たんぱく質LumBに目的のペプチドを融合させてディスプレーしようというものである。残念ながら、これらのグラム陰性および陽性菌における手法は、いずれもディスプレーできる目的たん

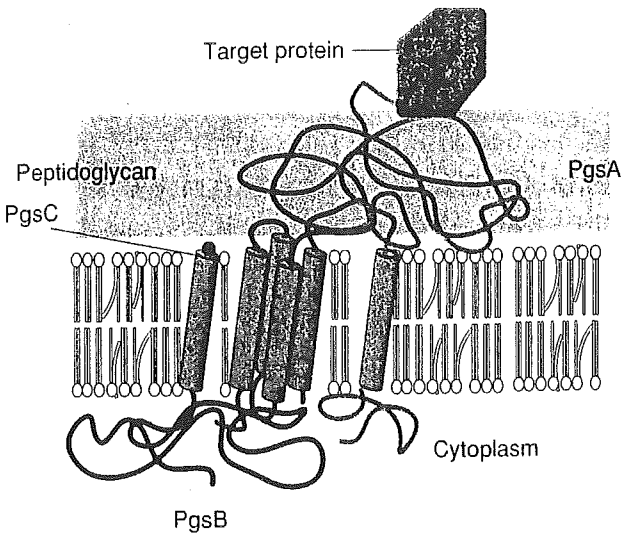

Fig 4　グラム陰性および陽性菌で有効な表層ディスプレーシステム

ぱく質は比較的小さなものに限られており、適用範囲に制約があった。

我々は、この問題点を解決するために、グラム陰性および陽性菌のいずれでも利用可能な新たな細胞表層ディスプレーシステムを、バイオベンチャーのバイオリーダースジャパン（大阪市）と共同で開発した。すなわち納豆菌に代表されるBacillus属細菌（Bacillus subtilisなど）によって生産されるポリγ-グルタミン酸の生合成にかかわる酵素複合体であるPgsABC（目的たんぱく質遺伝子を融合するPgsAは、全長379アミノ酸残基からなりN-末端とC-末端に特異的な疎水性アミノ酸配列を有している）をアンカーとして利用する方法を開発した（Fig 4）。

PgsABCは①細胞表層に多量に発現されていること②細胞周期上、休止期でも安定に維持されること③たんぱく質のアミノ酸１次配列と構造上の特性――など、外来たんぱく質を細胞表層へ発現させるための足場として利用するアンカーに求められる、多くの長所をもっていることが確認されている。PgsABCアンカーは、LPXTGモチーフを有する既存のアンカーとは異なり、その構造上の特徴から外来たんぱく質をそのC-末端に融合し、細胞表層に発現させることが可能である。

またPgsABCアンカーは、グラム陰性菌の大腸菌およびグラム陽性菌の乳酸菌において、70kDa以上の大きなたんぱく質を高密度に細胞表層ディスプレーできることが明らかになっており、細菌の細胞表層ディスプレー系の可能性を大きく広げるものと期待される。さらに最近、アンカーとしてはPgsAだけで十分であることも分かってきており、より広範囲な応用ができるものと期待されている。

高機能なバイオ素子を創出へ

cDNAライブラリーあるいはエラープローンPCR（ポリメラーゼ連鎖反応）やDNAシャッフリングなどの手法により、人工的に多様化した遺伝子群がコードするたんぱく質を細胞表層にディスプレーすることで、細胞表層ライブラリーを構築し、新しい機能性バイオ素子を創出することができる。機能性バイオ素子を細胞表層にディスプレーした場合、細胞外に位置することから、迅速に機能評価できる。

また、表層にある機能性バイオ素子と、細胞がもつ遺伝子は対応する形である（表現型と遺伝子型が一致している）ため、目的機能をもった細胞をスクリーニングすることで、目的バイオ素子（すなわちそれをコードする遺伝子）を得ることができる。ここで細胞を利用する場合、フローサイトメーター（FACS）による解析が可能となる点でメリットが大きい。蛍光標識した標的分子を用い、蛍光を発する細胞（すなわち標的分子が結合）をFACSで選択することで、標的分子に親和性をもつバイオ素子をハイスループットで探索できる。

さらに、ナノテクノロジーを駆使して作製されるチップ上に、ライブラリーを表層ディスプレーした酵母を配列させる「セルチップ」にすることで、シングル細胞レベルで相互作用を解析することもできる。また、基質をうまくデザインして、酵素分解産物が蛍光を発して細胞表層に結合できるようにすることで、目的触媒活性をもつ細胞、つまり酵素の探索もFACSやセルチップを用いてできる。新たに生み出された新機能性バイオ素子は、その遺伝子を取り出して様々に利用できるが、表層ディスプレーした微生物そのものを、新機能性をもった細胞として利用することも可能である。

細胞表層ディスプレーは、新機能性細胞およびバイオ素子の創出において大きな可能性を秘めた技術であると言える。また、創薬における有力なツールとしての開発も進んでいる。こうしたことからアイデアしだいで、生命科学研究に新たな道を開くとともに、革新的な応用が生まれるものと期待される。

Cell Transplantation, Vol. 14, pp. 647–653, 2005

0963-6897/05 $20.00 + .00
E-ISSN 1555-3892
www.cognizantcommunication.com

Differentiation of Adult Hepatic Stem-Like Cells Into Pancreatic Endocrine Cells

Satoko Yamada,* Kunihiko Terada,† Yasuharu Ueno,† Toshihiro Sugiyama,† Masaharu Seno,‡ and Itaru Kojima*

*Institute for Molecular and Cellular Regulation, Gunma University, Maebashi 371-8512, Japan
†Department of Biochemistry, Akita University School of Medicine, Akita 010-8543, Japan
‡Department of Bioscience and Biotechnology, Graduate School of Natural Science and Technology, Okayama University, Okayama 700-8530, Japan

To apply cell transplantation for treatment of diabetes mellitus, a sufficient number of β-cell sources are required. In the present study, we examined whether an epithelial cell line obtained from normal adult rat liver, namely hepatic stem-like (HSL) cells, which can be converted to both hepatocytes and billiary epithelial cells, could be a potential β-cell source. The growth speed of HSL cells was rapid and these cells were easily expanded in vitro. Bipotential hepatic stem cells, HSL cells, also expressed PGP9.5, which is expressed in neurons, β-cells, and progenitor cells of the pancreatic endocrine cells as well. Sodium butyrate induced morphological changes in HSL cells and converted them into flattened cells with large cytoplasm. When HSL cells were incubated with a combination of 5 mM sodium butyrate and 1 nM betacellulin, most of the cells were converted into morphologically neuron-like cells. RT-PCR analysis revealed that a series of transcriptional factors involved in differentiation of pancreatic endocrine cells was induced by the treatment with sodium butyrate and betacellulin. mRNAs for insulin, pancreatic polypeptide, and somatostatin were also observed. Immunoreactive pancreatic polypeptide, somatostatin, and insulin were detected in sodium butyrate and betacellulin-treated HSL cells. In conclusion, HSL cells obtained from adult normal liver also have the potential to differentiate into pancreatic endocrine cells in vitro. HSL cells may be one of the potential β-cell sources for cell transplant therapy for insulin-dependent diabetes.

Key words: Hepatic stem-like cell; Liver epithelial cell; Endocrine cell differentiation; Insulin

INTRODUCTION

Islet transplantation has been considered to be a new therapeutic option for the treatment of type 1 diabetes. In particular, use of nonsteroidal immunosuppressant markedly improve the outcome of islet transplantation (16,19), which has made this therapeutic approach quite attractive. The number of patients with diabetes greatly exceeds the number of pancreata obtained from cadaveric donors. A limited number of donors may be a limiting factor in performing islet transplantation. If β-cells are obtained by inducing differentiation of stem cells, it would be advantageous for realization of β-cell transplantation. In this regard, pancreatic ductal cells have been shown to convert to insulin-producing β-cells in vitro (1,15). Also, extrapancreatic stem cells (e.g., those from the liver, intestine, and the salivary gland) differentiate in vitro into insulin-producing cells under appropriate conditions (6,14,20,24). These results have shown that β-cells can be obtained in vitro from various types of progenitor cells. Two issues are particularly important to achieve cells for β-cell transplantation by means of in vitro conversion of stem cells. First, a large number of differentiated β-cells are necessary to control glucose metabolism in diabetic patients. Second, differentiated β-cells are thought to have fairly good responsiveness to glucose and incretin hormones. In this context, the use of progenitor cells is recommended because they can be obtained relatively easily and can be expanded easily in a culture system.

Hepatic stem-like (HSL) cells are epithelial cells obtained from adult rat liver (13). They have a cobblestone-like morphology typical of epithelial cells and express α-fetoprotein (13). When these cells are cocultured with hepatic stellate cells, they differentiate into albumin-expressing hepatocytes (13). Interestingly, these cells also differentiate into billiary epithelial cells when cultured with bile acid (unpublished). Therefore, HSL

Address correspondence to Itaru Kojima, M.D., Institute for Molecular and Cellular Regulation, Gunma University, Maebashi 371-8512, Japan. Tel: 81-27-220-8835; Fax: 81-27-220-8893; E-mail: ikojima@showa.gunma-u.ac.jp

cells are capable of differentiation into two types of liver cells: hepatocytes and billiary epithelial cells. Given that the liver and pancreas are derived from forgut epithelium (8), and stem cells in the two organs can differentiate into cells in the organ of the other (3,21,24,26), it is possible that HSL cells also differentiate into pancreatic endocrine cells. The present study was conducted to examine whether or not HSL cells also differentiate into pancreatic endocrine cells.

MATERIALS AND METHODS

Isolation and Culture of Cells

Rat HSL cells were isolated from 6- to 9-week-old male Sprague-Dawley rats as described by Nagai et al. (13) and maintained in Dulbecco's modified Eagle's medium (DMEM) with 4500 mg/L glucose (Invitrogen Corp, Carlsbad, CA) and 10% fetal bovine serum (FBS). Cells were used after 20–40 passages.

The experimental protocols were approved by the Animal Care and Ethical Committee of the Institute for Molecular and Cellular Regulation, Gunma University.

Measurement of Cell Proliferation and Morphological Examination

To measure cell growth, the cells were plated at a density of 1×10^4 cells/35-mm dish in DMEM containing 10% FBS. The number of viable cells was determined using 3-(4,5-dimethythiazol-2yl)-2,5-diphenyltetrazolimn bromide (MTT) as described by Carmichael et al. (2).

Morphological changes were observed with a phase contrast microscope (Olympus, Tokyo, Japan).

Immunofluorescence Study

HSL cells were cultured on noncoated glass coverslips at a density of 10^5 cells/ml. After overnight culture, cells were treated for 2 days with various factors. Cells were fixed with 3% paraformaldehyde in PBS, treated with 0.1% (v/v) Triton X-100 in PBS for 5 min, and incubated sequentially with Blocking Ace (Morinaga, Tokyo, Japan). Subsequently, primary antibody was applied for 1 h at room temperature; cells were washed with PBS and then incubated for 1 h at room temperature with a second antibody. The counterstaining was done with 4′,6-diamidino-2-phenylindol-HCl (DAPI) (Boehringer Mannheim, Mannheim, Germany). Finally, the sections were mounted with PermaFluor Aqueous Mounting Medium (IMMUNON Thermo Shandon, Pittsburg, PA). Cells were observed with an AX70 epifluorescence microscope (Olympus) equipped with a PXL 1400 cooled-charge-coupled device camera system (Photometrics, Tucson, AZ) operated with IP Lab Spectrum software (Signal Analysis, Vienna, VA).

Sources of Antibodies

Sources of the primary antibodies and the dilutions were as follows: rabbit anti-bovine keratin for wide spectrum screening (Ckwss), 1:1000 (DAKO Corp., CA, USA); mouse anti-human CK7, 1:50 (DAKO); mouse anti-human CK19, 1:100 (DAKO); rabbit anti-glucose transporter 2 (GLUT2), 1:50 (Biogenesis Ltd., UK); rabbit anti-human PGP9.5, 1:400 (Ultraclone Ltd., UK); rabbit anti-PDX-1, 1:250 (Transgene, Kumamoto, Japan); guinea pig anti-porcine insulin, 1:1000 (a generous gift from Dr. T. Matozaki of Gunma University); rabbit anti-human pancreatic polypeptide, 1:1000 (Chemicon); and rabbit anti-human somatostatin, 1:500 (DAKO).

Sources of the second antibodies and the dilutions were as follows: goat Alexa Fluor 488-cojugated anti-rabbit IgG, 1:400; goat Alexa Fluor 568-cojugated anti-rabbit IgG, 1:1000; goat Alexa Fluor 488-conjugated anti-guinea pig IgG, 1:400 (Molecular Probes, Inc., Eugene, OR). For CK7 and CK19, a Vectastain Elite ABC kit was used according to the manufacturer's recommendation.

Reverse Transcription-Polymerase Chain Reaction (RT-PCR)

Total RNA was extracted from the cells treated with or without sodium butyrate and/or betacellulin (BTC) using TRIzol Reagent (Invitrogen). RNA samples were pretreated with DNase I (Invitrogen) to remove contamination of genomic DNA. First-strand cDNA was synthesized by SuperScript II or SuperScript III RNaseH-Reverse Transcriptase (Invitrogen). To confirm no contamination of genomic DNA, samples without reverse transcriptase (RT) treatment were prepared. Oligonucleotide primers used and reaction conditions performed in this study were as previously described (11,27), except for NeuroD/Beta2 (5′-GGA CAA ACC TTT GCA GAG GAC GAG TGT CTG-3′ and 5′-AGC CAT GAA TGC AGA GGA GGA C-3′, initial denaturation at 95°C for 5 min followed by 33 cycles of 94°C for 30 s, 60°C for 45 s, 72°C 45 s), ngn3 (5′-AAG TGT CCC AAG AGA CCC AG-3′ and 5′-AGG CTA CCA GCT TGG GAA AC-3′, 36 cycles of 94°C for 30 s, 49°C for 30 s, 68°C for 30 s), insulin (5′-GGC TTT TGT CAA ACA GCA CCT TTG -3′ and 5′-CTC CAG TGC CAA GGT CTG AA-3′, 33 cycles of 94°C for 30 s, 58°C for 30 s, 68°C for 30 s), and somatostatin (5′-TCT CTG CTG CCT GCG GAC CT-3′ and 5′-GCC AAG AAG TAC TTG GCC AGT TC-3′, 35 cycles of 94°C for 30 s, 55°C for 30 s, 68°C for 30 s). The PCR products were subjected to 2% agarose gel electrophoresis and visualized by staining with ethidium bromide. An insulin PCR product was confirmed by sequencing using an ABI Prism Dye Terminator Cycle Sequencing FS Ready Reaction Kit and

ABI Prism 377 DNA sequencer (Applied Biosystems, Foster City, CA).

Materials

Sodium butyrate and trichostatin A were purchased from Sigma (St. Louis, MO). Recombinant human BTC was prepared as described previously (17).

RESULTS

Evaluation of Proliferation of HSL Cells

We first determined the proliferation rate of HSL cells by using MTT. As shown in Figure 1, the growth rate of HSL cells was rapid. Figure 2A depicts a cobblestone-like appearance of HSL cells.

Effects of Sodium Butyrate and Betacellulin on Morphological Changes in HSL Cells

To assess whether HSL cells have the possibility to differentiate into endocrine cells, we screened various differentiation and growth factors in an in vitro culture system. Among the various factors tested, sodium butyrate induced morphological changes as shown in Figure 2B. The majority of HSL cells treated with 5 mM sodium butyrate became flattened with large cytoplasm. Some of the cells changed into spindle-like shaped cells. All of these cells expressed cytokeratin 7 and 19 (data not shown). BTC (1 nM), a growth factor originally isolated from the conditioned medium of insulin-producing tumor cells (βTC) (18) and now also well known as a β-cell differentiation factor (11), converted most of the HSL cells into spindle-shaped cells when added with sodium butyrate (Fig. 2C). The cell number of HSL cells decreased to 60–70% on average after the treatment with sodium butyrate and BTC for 48 h.

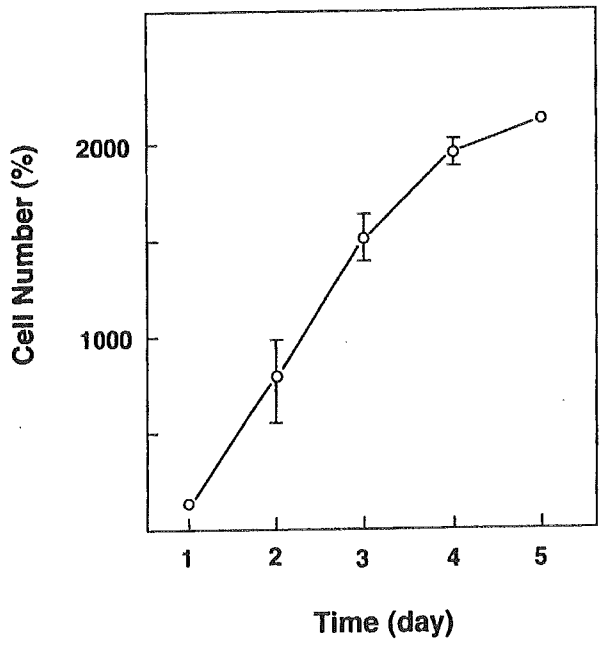

Figure 1. Growth curve of HSL cells. HSL cells were cultured in DMEM containing 10% FCS, and changes in the number of viable cells were measured by using MTT.

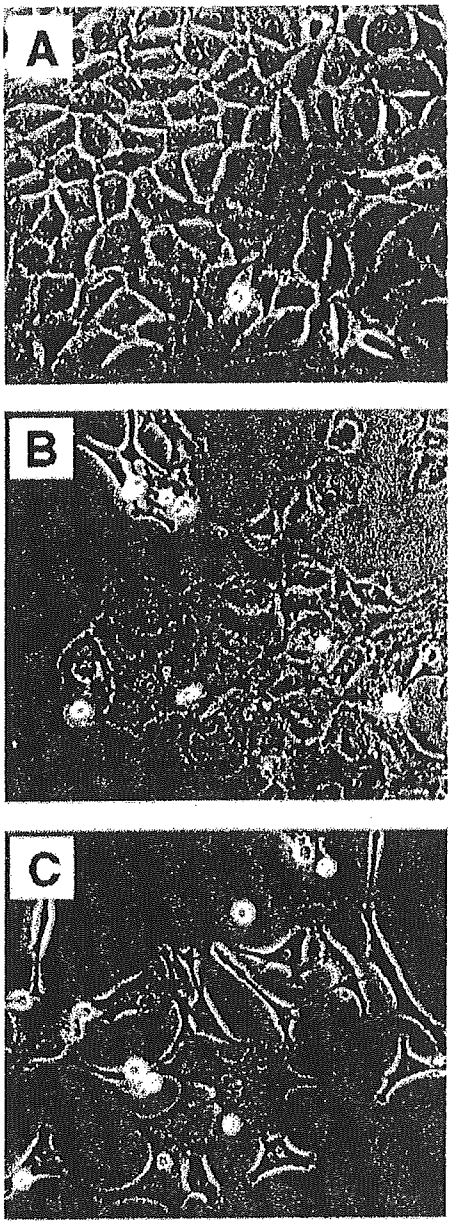

Figure 2. Morphological changes in HSL cells treated with sodium butyrate and BTC. HSL cells were incubated in DMEM with 5 mM sodium butyrate (B) or 5 mM sodium butyrate and 1 nM BTC (C) for 48 h. Morphological changes were observed by phase-contrast microscopy. Nontreated HSL cells are shown in (A). Original magnification: ×200.

HSL Cells Differentiated Into Pancreatic Polypeptide-, Somatostatin-, and Insulin-Expressing Endocrine Cells

Next we evaluated the characteristics of HSL cells treated with sodium butyrate and BTC by RT-PCR and immunocytochemistry. As previously reported, HSL cells expressed stem cell markers including c-kit, Musashi-1, and hepatoblast marker α-feteprotein (12,13). HSL cells also expressed PGP9.5, which is known as a neuron marker and a marker for pancreatic progenitor cells (25) (Fig. 3A). PGP9.5 expression was upregulated when treated with sodium butyrate and BTC. Treatment of HSL cells with sodium butyrate and BTC induced the expression of PDX-1, which is a key transcription factor in the pancreas development and hepato-pancreatic transdifferentiation (4,7). Accordingly, a series of transcriptional factors expressed during pancreatic development (i.e., NeuroD/Beta2, Nkx2.2, Nkx6.1, and Pax6) was newly expressed. In addition, Pax4 and Isl-1 were upregulated by the treatment (Fig. 3A). Ngn3, which is transiently expressed when cells are directed for endocrine cell fate (22), began to be expressed at 6 h, and was maximally expressed at 48 h after the treatment with sodium butyrate and BTC (Fig. 3B). Sodium butyrate and BTC induced the expression of pancreatic endocrine hormone, somatostatin, pancreatic polypeptide, and insulin, although their expression levels were low (Fig. 3A).

Immunocytochemical examination showed that sodium butyrate and BTC induced PGP9.5 and PDX-1. GLUT2 was scarcely detected in naive HSL cells, but its expression was detected after the treatment with sodium butyrate and BTC (data not shown). Ckwss was also expressed in naive and treated HSL cells. Pancreatic en-

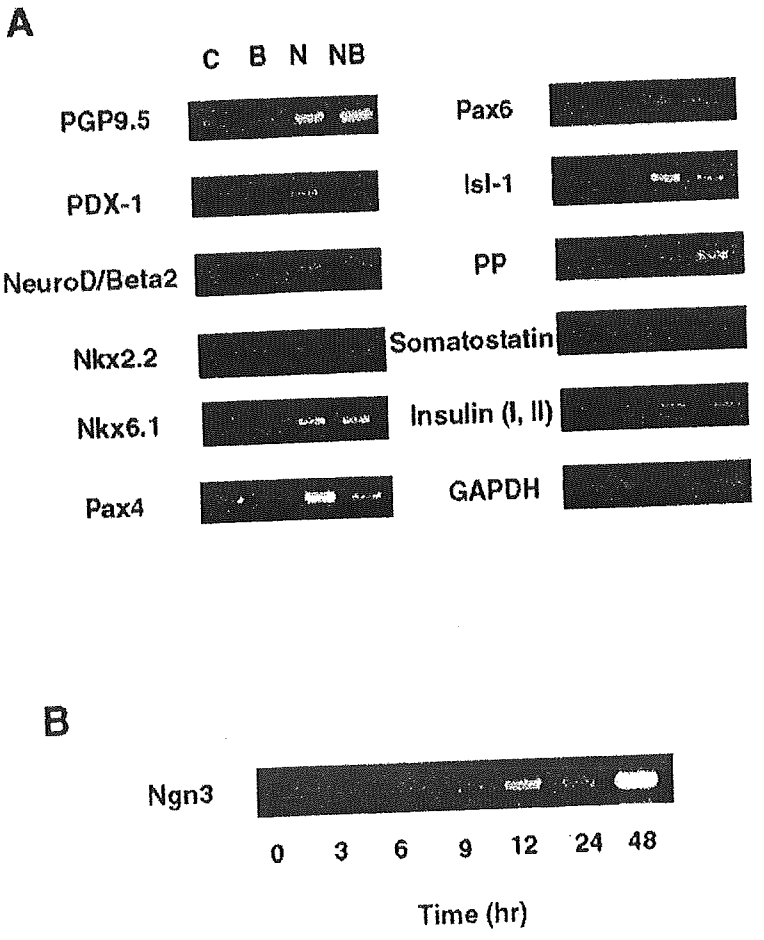

Figure 3. Induction of the expression of pancreas-related markers and pancreatic hormones in HSL cells. (A) HSL cells were treated for 48 h with or without 5 mM sodium butyrate and/or 1 nM BTC. mRNA for PGP9.5, transcription factors, hormones, and GAPDH was measured by RT-PCR. GAPDH served as an internal standard. C, control; B, 1 nM BTC, N, 5 mM sodium butyrate, NB, 5 mM sodium butyrate and 1 nM BTC. (B) HSL cells were treated for 3, 6, 9, 12, 24, and 48 h with 5 mM sodium butyrate and 1 nM BTC. mRNA for ngn3 was measured by RT-PCR.

docrine hormones, PP, somatostatin, and insulin were also detected at protein levels but their levels were low (Fig. 4).

DISCUSSION

In the present study, we demonstrated that adult hepatic stem-like cells have potential to differentiate into pancreatic endocrine cells in vitro. It was shown that hepatic oval cells can differentiate into pancreatic endocrine cells when cultured in a high glucose environment (24). Both oval cells and HSL cells express stem cell marker c-kit and hepatoblast marker α-fetoprotein and differentiate into hepatocytes and cholangiocytes. On the other hand, oval cells also express albumin and CK19, markers of hepatocytes and billiary epithelial cells, respectively. However, HSL cells do not express these two markers. Moreover, HSL cells express neuronal and gastrointestinal stem cell marker Musashi-1 (12) and, in addition, we showed that they also express PGP9.5, a putative marker of pancreatic progenitor cells (25). Based on these observations, we consider that HSL cells might be more immature, pluripotent hepatic stem cells compared to oval cells, and HSL cells may be capable of converting to pancreatic endocrine cells.

Of the various factors tested, a histone deacetylase inhibitor sodium butyrate induced morphological changes in HSL cells and converted them to flattened cells with large cytoplasma. Sodium butyrate also induced the expression of various transcription factors involved in differentiation of pancreatic cells. Additionally, cells treated with sodium butyrate expressed CK19 and CK7 (data not shown). These observations indicate that differentiated cells expressed both ductal and endocrine markers. Trichostatin A, another inhibitor of histone deacetylase (23), mimicked the effect of sodium butyrate (data not shown). Although sodium butyrate had pleiotropic actions (9), it is likely that inhibition of histone deacetylase activity may have accounted for the induction of differentiation by sodium butyrate. The effect of BTC in sodium butyrate-treated cells was not so evident at the mRNA level. The addition of BTC, however, changed most of the HSL cells from round-shaped flattened cells to spindle-like cells, and immunoreactivity of the pancreatic hormones became detectable by the addition of BTC.

HSL cells are considered to be closely related to WB-F344 cells (5). Both are isolated from adult rat liver and are regarded as "liver epithelial cells." WB-F344 cells were shown to differentiate into myocytes in the heart

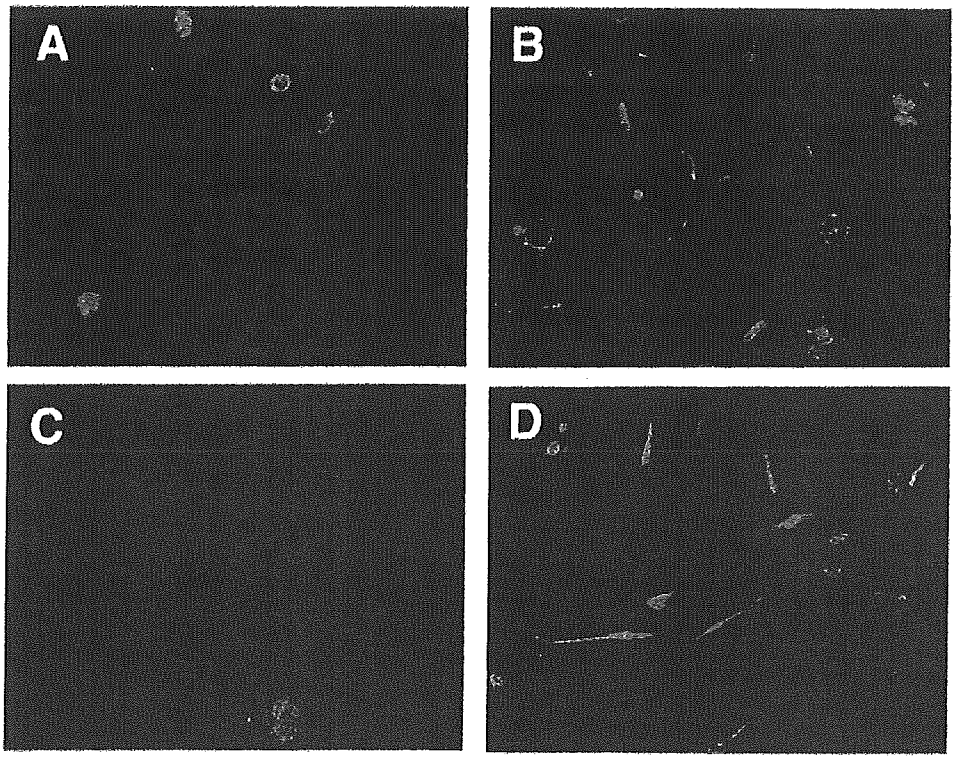

Figure 4. Immunocytochemistry of HSL cells treated with sodium butyrate and BTC. HSL cells were incubated for 48 h with a combination of 5 mM sodium butyrate and/or 1 nM BTC. Cells were stained with anti-PDX-1 (A), or anti-PP (B), or anti-somatostatin (C), or anti-insulin (D) antibody. Original magnification: ×200.

in vivo, beyond the hurdle between endoderm and mesoderm (10).

As shown in Figure 1, HSL cells proliferate quite rapidly and the cell number can be easily expanded in vitro. HSL cells were obtained from adult liver in normal rat. This is in contrast to oval cells, which are not readily available from normal liver. Consequently, HSL cells are advantageous for their availability. Indeed, it is quite likely that a similar type of cells may exist in human liver.

Given their growth property and differentiation potential, such cells are advantageous for use in future cell therapy to treat diabetes. It should be mentioned that although we could convert HSL cells to insulin-producing cells in vitro, the maturity of the differentiated cells is still low. Further study is clearly needed to determine the conditions to fully differentiate these cells to pancreatic β-cells.

ACKNOWLEDGMENTS: The authors are grateful to Mayumi Odagiri for secretarial assistance. The present study was supported by a Grant-in-Aid for Scientific Research from the Ministry of Education, Science, Sports and Culture of Japan and a grant from the Project for Realization of Regeneration Medicine.

REFERENCES

1. Bonner-Weir, S.; Taneja, M.; Weir, G. C.; Tatarkiewicz, K.; Song, K. H.; Sharma, A.; O'Neil, J. J. In vitro cultivation of human islets from expanded ductal tissue. Proc. Natl. Acad. Sci. USA 97:7999–8004; 2000.
2. Carmichael, J.; DeGraff, W. C.; Gazdar, A. F.; Minam, J. D.; Mitchell, J. B. Evaluation of tetrazolium-based semiautomated colorimetric assay. Cancer Res. 47:936–942; 1987.
3. Chen, J. R.; Tsao, M. S.; Duguid, W. P. Hepatocytic differentiation of cultured rat pancreatic ductal epithelial cells after in vivo implantation. Am. J. Pathol. 147:707–717; 1995.
4. Ferber, S.; Halkin, A.; Cohen, H.; Ber, I.; Einav, Y.; Goldberg, I.; Barshack, I.; Seijffers, R.; Kopolovic, J.; Kaiser, N.; Karasik, A. Pancreatic and duodenal homeobox gene 1 induces expression of insulin genes in liver and ameliorates streptozotocin-induced hyperglycemia. Nat. Med. 6: 568–572; 2000.
5. Grisham, J. W.; Coleman, W. B.; Smith, G. J. Isolation, culture, and transplantation of rat hepatocytic precursor (stem-like) cells. Proc. Soc. Exp. Biol. Med. 204:270–279; 1993.
6. Hisatomi, Y.; Okumura, K.; Nakamura, K.; Matsumoto, S.; Satoh, A.; Nagano, K.; Yamamoto, T.; Endo, F. Flow cytometric isolation of endodermal progenitors from mouse salivary gland differentiate into hepatic and pancreatic lineages. Hepatology 39:667–675; 2004.
7. Horb, M. E.; Shen, C. N.; Tosh, D.; Slack, J. M. Experimental conversion of liver to pancreas. Curr. Biol. 13: 105–115; 2003.
8. Jensen, J. Gene regulatory factors in pancreatic development. Dev. Dyn. 229:176–200; 2004.
9. Kruh, J. Effects of sodium butyrate, a new pharmacological agent, on cells in culture. Mol. Cell. Biochem. 42:65–82; 1982.
10. Malouf, N. N.; Coleman, W. B.; Grisham, J. W.; Lininger, R. A.; Madden, V. J.; Sproul, M.; Anderson, P. A. Adult-derived stem cells from the liver become myocytes in the heart in vitro. Am. J. Pathol. 158:1929–1935; 2001.
11. Mashima, H.; Ohnishi, H.; Wakabayashi, K.; Mine, T.; Miyagawa, J.; Hanafusa, T.; Seno, M.; Yamada, H.; Kojima, H. Betacellulin and activin A coordinately convert amylase-secreting pancreatic AR42J cells into insulin-secreting cells. J. Clin. Invest. 97:1647–1654; 1996.
12. Miura, K.; Nagai, H.; Ueno, Y.; Goto, T.; Mikami, K.; Nakane, K.; Yoneyama, K.; Watanabe, D.; Terada, K.; Sugiyama, T.; Imai, K.; Senoo, H.; Watanabe, S. Epimorphin is involved in differentiation of rat hepatic stem-like cells through cell-cell contact. Biochem. Biophys. Res. Commun. 311:415–423; 2003.
13. Nagai, H.; Terada, K.; Watanabe, G.; Ueno, Y.; Aiba, N.; Shibuya, T.; Kawagoe, M.; Kameda, T.; Sato, M.; Senoo, H.; Sugiyama, T. Differentiation of liver epithelial (stem-like) cells into hepatocytes induced by coculture with hepatic stellate cells. Biochem. Biophys. Res. Commun. 293:1420–1425; 2002.
14. Okumura, K.; Nakamura, K.; Hisatomi, Y.; Nagano, K.; Tanaka, Y.; Terada, K.; Sugiyama, T.; Umeyama, K.; Matsumoto, K.; Yamamoto, T.; Endo, F. Salivary gland progenitor cells induced by duct ligation differentiate into hepatic and pancreatic lineages. Hepatology 38:104–113; 2003.
15. Ramiya, V. K.; Maraist, M.; Arfors, K. E.; Schatz, D. A.; Peck, A. B.; Gornelius, J. G. Reversal of insulin-dependent diabetes using islets generated in vitro from pancreatic stem cells. Nat. Med. 6:278–282; 2000.
16. Robertson, R. P. Islet transplantation as a treatment for diabetes—a work in progress. N. Engl. J. Med. 350:694–705; 2004.
17. Seno, M.; Tada, H.; Kosaka, M.; Sasada, R.; Igarashi, K.; Shing, Y.; Folkman, J.; Ueda, M.; Yamada, H. Human betacellulin, a member of EGF family dominantly expressed in pancreas and intestine, is fully active in a monomeric form. Growth Factors 13:181–191; 1996.
18. Shing, Y.; Christofori, G.; Hanahan, Y.; Ono, R.; Sadada, R.; Igarashi, K.; Folkman, J. Betacellulin: A mitogen from pancreatic β cell tumors. Science 259:1604–1607; 1993.
19. Stock, P. G.; Bluestone, J. A. Beta-cell replacement for type I diabetes. Annu. Rev. Med. 55:133–156; 2004.
20. Suzuki, A.; Nakauchi, H.; Taniguchi, H. Glucagon-like peptide 1 (1-37) converts intestinal epithelial cells into insulin-producing cells. Proc. Natl. Acad. Sci. USA 100: 5034–5039; 2003.
21. Tosh, D.; Shen, C. N.; Slack, J. M. W. Conversion of pancreatic cells to hepatocytes. Biochem. Soc. Trans. 30: 51–54; 2002.
22. Watada, H. Neurogenin 3 is a key transcription factor for differentiation of the endocrine pancreas. Endocr. J. 51: 255–264; 2004.
23. Wu, J. T.; Archer, S. Y.; Hinnebusch, B.; Meng, S.; Hodin, R. A. Transient vs. prolonged histone hyperacetylation: Effects on colon cancer growth, differentiation, and apoptosis. Am. J. Physiol. 280:G482–G490; 2001.
24. Yang, L.; Li, S.; Hatch, H.; Ahrens, K.; Cornelius, J. G.; Petersen, B. E.; Peck, A. B. In vitro trans-differentiation of adult hepatic stem cells into pancreatic endocrine hormone-producing cells. Proc. Natl. Acad. Sci. USA 99: 8078–8083; 2002.
25. Yokoyama-Hayashi, K.; Takahashi, T.; Kakita, A.; Yamashina, S. Expression of PGP9.5 in ductal cells of the rat pancreas ducing development and regeneration: Can it

be a marker for pancreatic progenitor cells? Endocr. J. 49: 51–74; 2002.

26. Zalzman, M.; Gupta, S.; Girl, R. K.; Berkovich, I.; Sappal, B. S.; Karnieli, O.; Zern, M. A.; Fleischer, N.; Efrat, S. Reversal of hyperglycemia in mice by using human expandable insulin-producing cells differentiated from fetal liver progenitor cells. Proc. Natl. Acad. Sci. USA 100: 7253–7258; 2003.
27. Zhang, Y. Q.; Mashima, H.; Kojima, I. Changes in the expression of transcription factors in pancreatic AR42J cells during differentiation into insulin-producing cells. Diabetes 50:S10–S14; 2001.

Available online at www.sciencedirect.com
SCIENCE DIRECT®
Biochemical and Biophysical Research Communications 334 (2005) 263–268
BBRC
www.elsevier.com/locate/ybbrc

Identification of cell surface marker candidates on SV-T2 cells using DNA microarray on DLC-coated glass

Tuoya [a], Koichi Hirayama [b], Tadahiro Nagaoka [a], Dongwei Yu [a], Takayuki Fukuda [a,c], Hiroko Tada [a], Hidenori Yamada [a], Masaharu Seno [a,d,*]

[a] *Graduate School of Natural Science and Technology, Okayama University, Okayama 700-8530, Japan*
[b] *Toyo Kohan Co., Ltd., Yamaguchi 744-8611, Japan*
[c] *Kobe R&D Center, Katayama Chemical Industries Co., Ltd., Hyogo 650-0047, Japan*
[d] *Research Center for Biomedical Engineering, Okayama University, Okayama 700-8530, Japan*

Received 14 June 2005
Available online 27 June 2005

Abstract

We analyzed gene expression profiles of normal mouse fibroblast BALB/c 3T3 cells and its SV40 transformant SV-T2 cells using our originally developed cell surface marker DNA microarray, which is prepared on a diamond-like carbon-coated glass. As a result, CD62L and IL-6 receptor α gene expressions were upregulated in SV-T2 and were thought to be candidates for cell surface markers of the cells. The result of microarray analysis was validated by real-time quantitative PCR, immunohistochemistry and biological assays. These data show that our cell surface marker DNA microarray should be useful in finding the candidates of cell type-specific surface markers.

Keywords: Cell surface marker; DNA microarray; DLC-coated glass; BALB/c 3T3 cells; SV-T2 cells; IL-6 receptor α

Cell surface proteins are involved in biological functions, such as cell surface receptors, growth factor receptors, and cell adhesion molecules. Further, it has been found that there is a difference in their gene expression between tumor and corresponding adjacent normal tissue [1]. This heterogeneity of cell surface protein expression makes these molecules useful markers for specific tumor targeting [2–6]. Therefore, it would be extremely desirable to distinguish the cells or tissues in some diseases from those in a normal state by cell or tissue-specific surface markers.

To identify cell-specific surface markers, DNA microarray technology would be the best candidate, since large-scale, high-throughput screening of the expressing genes are possible at one time, whereas Northern hybridization or RT-PCR procedures are designed only for the characterization of the target genes.

The use of DNA microarray to determine gene expression has grown significantly during the last 10 years. Sophisticated data analysis has already demonstrated that various tumor types can be distinguished on the basis of their gene expression patterns, and a large number of genes are overexpressed in tumor compared to their normal tissue counterparts [7]. However, it still appears difficult to show reliable and reproducible results, depending on the density and the method of immobilization of spotted probe DNAs. In view of this, we employed diamond-like carbon (DLC)-coated glass to design an original DNA microarray. Since DLC coating can provide a high density of activated carbon atoms to covalently conjugate DNAs, reliable results could be expected.

The probe design should also be very carefully organized because various kinds of heterogeneity are present

* Corresponding author. Fax: +81 86 251 8216.
E-mail address: mseno@cc.okayama-u.ac.jp (M. Seno).

0006-291X/$ - see front matter © 2005 Elsevier Inc. All rights reserved.
doi:10.1016/j.bbrc.2005.06.083

by alternative splicing even in a single gene [8]. In many cases, gene families contain a wide expansion of molecules so that various designs of probes of genes should be used to expect the results in high precision. Instead of using as many probes as possible, another idea would be to organize a microarray with probes in a category, such as cell surface markers. Simultaneously, artificial RNA and its complementary DNA would be helpful to verify the procedure, if the sequence has no homology to any described human, mouse, or rat genes.

As a result, we designed an original DNA microarray and tried to characterize normal mouse fibroblast BALB/c 3T3 cells and its SV40 transformant SV-T2 cells.

Materials and methods

Reagents and Antibodies. IL-6 was from Wako Pure Chemical Industries (Japan). Anti-EGFR, anti-CD11b (anti-integrinαM) and anti-IL-6Rα antibodies were from Santa Cruz Biotechnology (CA). Anti-CD62L was from Southern Biotechnology Associates (AL). Anti-IL-6Rα neutralizing antibodies were from Innogenetics (Belgium).

Cell lines and cell cultures. Both mouse cell lines, BALB/c 3T3 and SV-T2, were maintained in DMEM supplemented with 10% (v/v) fetal bovine serum (FBS). For RNA isolation, SV-T2 cells were cultured on 0.5% bacto-agar (BD, NJ) to form colonies, while BALB/c 3T3 cells were cultured in a 100 mm dish.

Design of DNA microarray. We designed a DNA microarray that carries 60-mer oligonucleotide probes for 378 mouse cell surface proteins. This design of probes was implemented primarily to include the DNA sequence coding the transmembrane region or the GPI-anchor attachment site, which is the essential information for proteins to localize on the cell surface. The probes were synthesized with NH_2 radical at the 5′ end and spotted onto a DLC-coated glass slides, Gene Slide (Toyo Kohan, Japan). The surface of the Gene Slide was activated in advance at the carbon atoms and was ready to be conjugated with DNA by a covalent bond. The probes were spotted in quadruplicate, so that the intensity of signals for each gene could be analyzed statistically. This microarray included control spots complementary to the control RNA to verify coupling and hybridization described below.

RNA preparation. Total RNA was isolated from cells with the RNeasy Mini kit (Qiagen, Germany). After DNase treatment, the purity of RNA was assessed by the measurement of absorbance at 260 and 280 nm as the ratio of $OD_{260/280}$ at more than 1.4. Also, the integrity of RNA was determined by gel electrophoresis as the ratio of 28S/18S at more than 1.8. Genomic DNA contamination was tested by PCR with primers for GAPDH to amplify no visible product after 35 cycles.

Control RNA preparation. For in vitro synthesis of control RNA, we inserted a 756-bp fragment derived from EGFP cDNA sequence (GenBank Accession No. U76561) together with a poly(A)$_{24}$ downstream of the T7 promoter to construct a plasmid pBO795. The linear template for in vitro transcription with T7 RNA polymerase was prepared using the plasmid by PCR. The transcription reaction took place at 37 °C for 4 h. After DNase treatment and purification, the purity of the control RNA was assessed by measurement of absorbance at 260 and 280 nm and tested by PCR for template DNA as described in "RNA preparation."

DNA microarray assay. Twenty micrograms of total RNA from cells, together with 2 ng of control RNA, was used as the template of cDNA synthesis. Fluorescent-labeled cDNAs were prepared by reverse transcription of the mixtures in the presence of amino-allyl-dUTP followed by coupling of the Cy3 dye (Amersham Biosciences). The labeled cDNA was purified with the QIAquick PCR Purification Kit (Qiagen) and then used for hybridization at 55 °C for 15 h. The slides were washed and scanned using an FLA8000 scanner (Fuji Film, Japan). The intensity of each signal was analyzed with GenePix Pro 5.1 software (Axon). Gene expression levels were compared to one another by relative fluorescent intensity (RFI), where RFI is the percentage of the fluorescent intensity of each gene and considering that of the internal control to be 100%.

Real-time quantitative PCR. A half nanogram of internal control RNA was mixed with 5 μg of total RNA from each cell line, and reverse-transcribed for single-strand cDNAs using oligo(dT)$_{18}$ primer. Then real-time quantitative PCR (RT-qPCR) was performed using Light Cycler DX400 (Roche) with LightCycler FastStart DNA Master SYBR Green I kit (Roche) in triplicate. The PCR was 40 cycles of 10 s at 95 °C, 10 s at 60 °C, and 25 s at 72 °C. The melting curve analysis was 0 s at 95 °C, 15 s at 65 °C, up to 98 °C, and cooled to 40 °C. The primer pairs used were as follows: 5′-GCCCCAGTGTCAGTATGTGGT-3′ and 5′-GGGATGAATGAGCGAGGGGAA-3′ for CD62L, 5′-GCAGTTCCAGCTTCGATACCG-3′ and 5′-GTCATAAGGGCTCTGTGCGTC-3′ for IL-6Rα, 5′-CAGGGAGTGCGTGGAGAAATG-3′ and 5′-GCTCCCGAACCCAGAACTTTG-3′ for EGFR (GenBank Accession No. NM_007912), 5′-TGGAGCTGCCTGTGAAGTACG-3′ and 5′-TTACTGAGGTGGGGCGTCTTG-3′ for CD11b.

Immunofluorescence. Cells cultured in Lab-Tek chamber slides were washed with phosphate-buffered saline (PBS), fixed with 10% formalin and permeabilized with 0.2% Triton X-100 on the glass slides. Cells were then incubated with the primary antibody of each protein and second antibody IgG-FITC. Fluorescence images were collected on a Zeiss confocal microscope and photographed using a 63× immersion objective.

Cell growth assay. The cells were plated in 96-well plates. IL-6 and/or anti-IL-6Rα were added daily to maintain the concentration for 5 days. Cell growth was determined by 3-(4,5-dimethyl-thiazol-2-yl)-2,5-diphenyltetrazolium bromide (MTT) assay [9]. The relative cell growth for each treatment is expressed as a percentage of untreated control cultures. The statistical significance of differences between the means of six replicates was assessed by Student's t test, with $P < 0.05$ being considered significant.

Results and discussion

Gene expression profiling of BALB/c 3T3 and SV-T2 cells

In order to screen cell surface marker proteins differentially expressed in the two cell lines, we performed DNA microarray analysis. The results of our original mouse cell surface marker arrays on DLC-coated glass are summarized in Fig. 1. The scatter plot of the gene expression pattern between independent experiments on BALB/c 3T3 cells shows excellent reproducibility of the results with a correlation coefficient of 0.99 (Fig. 1A). When BALB/c 3T3 cells were compared to SV-T2 cells, no difference in the expression levels of almost 200–250 of 378 genes was found between the two cell lines. We chose 19 genes whose expression was considered significantly upregulated in SV-T2 cells when compared with BALB/c 3T3 cells, judging by the average difference in value of relative fluorescence intensity (RFI) greater than 20 (Fig. 1B, Table 1). In a similar

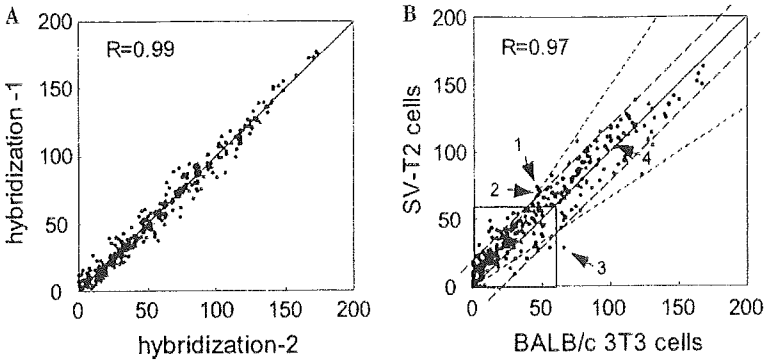

Fig. 1. Scatter plots of gene expression pattern. (A) Two independent hybridizations of BALB/c 3T3 cells are compared. (B) SV-T2 cells vs BALB/c 3T3 cells. The cutoffs for average difference values of relative fluorescence intensity (RFI) greater than 20 are indicated by dashed lines and 1.5-fold upregulated and downregulated are indicated by short dashed lines. Each arrowhead corresponds to the genes extracted in this study. (1) CD62L; (2) IL-6Rα; (3) CD11b; (4) EGFR.

Table 1
Genes significantly upregulated in SV-T2 cells

Gene	GenBank Accession	A[a]	B[a]	d_1[b]	t_1[c]
Asialoglycoprotein receptor 2	NM_007493	70.6	91.1	20.5	1.3
interleukin 12 receptor, beta 1	NM_008353	20.2	40.7	20.6	2.0
adrenergic receptor, beta 2	X15643	1.9	22.6	20.8	12.1
gap junction membrane channel protein alpha3	NM_016975	33.1	53.8	20.8	1.6
prostaglandin D receptor	NM_008962	49.3	70.3	21.0	1.4
neuromedin B receptor	NM_008703	93.2	114.6	21.4	1.2
interleukin 6 receptor, alpha (IL-6Rα)	X53802	48.8	71.0	22.3	1.5
integrin alpha 6	X69902	13.8	36.1	22.4	2.6
gap junction membrane channel protein beta 6	NM_008128	17.4	41.6	24.3	2.4
tumor-associated calcium signal transducer 1	NM_008532	57.7	82.4	24.6	1.4
contactin 3	NM_008779	29.3	54.3	25.1	1.9
glycophorin A	NM_010369	25.0	50.4	25.4	2.0
occludin	U49185	4.0	30.8	26.8	7.7
selectin, lymphocyte (CD62L)	NM_011346	46.7	74.2	27.5	1.6
platelet/endothelial cell adhesion molecule	L06039	11.1	40.5	29.4	3.6
glycoprotein 5 (platelet)	NM_008148	13.7	43.1	29.5	3.2
integrin beta 1 (fibronectin receptor beta)	Y00769	13.6	43.4	29.8	3.2
neuropeptide Y receptor Y6	NM_010935	76.5	107.2	30.7	1.4
interleukin 1 receptor, type I	M27960	12.2	48.5	36.3	4.0

[a] A and B denote RFIs in BALB/c 3T3 and SV-T2 cells, respectively.
[b] $d_1 = B - A$.
[c] $t_1 = B/A$.

Table 2
Genes significantly downregulated in SV-T2 cells

Gene	GenBank Accession	A[a]	B[a]	d_2[b]	t_2[c]
Burkitt lymphoma receptor 1	NM_007551	123.7	82.7	20.5	1.3
integrin alpha M (CD11b)	X07640	66.3	28.4	20.6	2.0
galanin receptor 1	Y15004	56.4	28.5	20.8	12.1
histamine receptor H 1	NM_008285	131.3	104.1	20.8	1.6
prostaglandin E receptor EP2 subtype	NM_008964	78.2	55.8	21.0	1.4
coagulation factor III	NM_010171	30.6	8.9	21.4	1.2
purinergic receptor P2X-like 1, orphan receptor	NM_011028	47.2	25.9	22.3	1.5
intercellular adhesion molecule	M31585	64.3	43.2	22.4	2.6

[a] A and B denote RFIs in BALB/c 3T3 and SV-T2 cells, respectively.
[b] $d_2 = A - B$.
[c] $t_2 = A/B$.

manner, eight downregulated genes are listed in Table 2. In order to pick up the candidates of the potential cell surface markers for ST-T2 cells, we tentatively applied the following two criteria to the 19 genes: (1) a ratio value of RFI in SV-T2 versus RFI in BALB/c 3T3 greater than 1.5, i.e., $B/A \geqslant 1.5$, where A and B represent RFI in BALB/c 3T3 and SV-T2 cells, respectively; (2) a value of RFI in SV-T2 greater than 60, i.e., $B > 60$, which is equivalent to the expression level of a housekeeping gene, GAPDH. Among the criteria, the first represents a significant increase, while the second represents an expression level that should be useful as an actual cell surface marker. Only two genes, IL-6Rα and CD62L, satisfied the criteria. Through inverse comparison, three genes, CD11b, Burkit lymphoma receptor 1 and intercellular adhesion molecule, satisfied the criteria (Table 2). Since CD11b showed the highest ratio of A/B and as the antibody was commercially available, further validation of this gene was carried out as the representative of the downregulated expression.

Confirmation of differentially expressed genes by real-time quantitative PCR

Real-time quantitative PCR analyses were used to validate top ranks of differentially expressed genes profiled by the microarray. IL-6Rα and CD62L were 11- and 300-fold upregulated in SV-T2 cells, respectively, while CD11b was less than 0.5-fold downregulated (Table 3). The level of CD11b expression in SV-T2 cells, which required more than 40 cycles of PCR amplification to be confirmed, was so low that the precise estimation of downregulation was difficult to accomplish by this method. As for the expression of the EGF receptor (EGFR) gene, the RFI of BALB/c 3T3 cells was 101.7 and that of SV-T2 cells was 108.3, which made the spot close to the 45° diagonal line in the scatter plot (Fig. 1B). We considered that the levels are almost equivalent and took this gene as representative of unchanged expression. As a result, our DNA microarray appears to be able to successfully detect expression change more than 10-fold.

Detection of candidates for cell surface markers by immunofluorescence

Next, we raised two questions of (a) whether the corresponding proteins are localized on the surface of the cells, and (b) whether the relative amount of the proteins on the two cell lines reflected the level of gene expression. We evaluated the protein expression of the four cell surface proteins by immunofluorescence (Fig. 2). In BALB/c 3T3 cells there was no positive staining or only faint staining for IL-6Rα and CD62L, while SV-T2 cells showed strong fluorescence. CD11b showed inverse results. EGFR were detected on the surface of both cell lines. These results are consistent with the results obtained by the microarray and RT-qPCR.

Table 3
Summary of RT-qPCR on the change in gene expression

Gene	SV-T2 cells relative to BALB/c 3T3 cells (folds)
CD62L	300.2 ± 23.6
IL-6Rα	10.8 ± 2.0
CD11b	0.5 ± 0.3
EGFR	4.4 ± 0.4

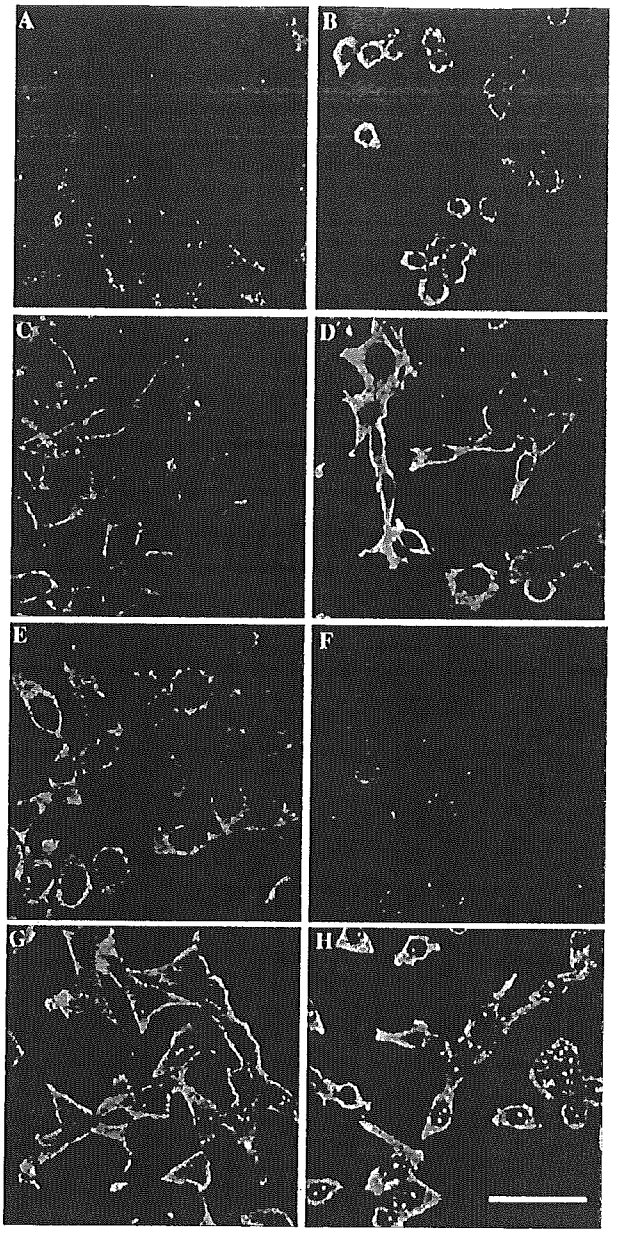

Fig. 2. Detection of cell surface proteins by immunofluorescence. BALB/c 3T3 cells (A,C,E,G) and SV-T2 cells (B,D,F,H) were immunostained with antibodies against CD62L (A,B), IL-6Rα (C,D), CD11b (E,F), and EGFR (G,H). Scale bar = 50 μm.

SV-T2 cells respond to IL-6 via IL-6Rα

Since we found that IL-6Rα was increased in SV-T2 cells, we assessed the sensitivity of these cells to IL-6. IL-6 is a pleiotropic cytokine that is implicated in a variety of cellular functions in immune, hematopoietic, neural, and hepatic systems. IL-6 has also been shown to influence the proliferation of normal and tumor-derived cells [10]. When the cells were treated with IL-6, the proliferation of SV-T2 cells was inhibited in a dose-dependent manner, while no effects were observed in BALB/c 3T3 cells (Fig. 3). IL-6 acts through the receptor complex that consists of an α chain subunit (i.e., IL-6Rα) with specific affinity for IL-6 and a β chain subunit of signal transducer known as gp130 without specific affinity to ligands [10,11]. RT-qPCR showed the expression of IL-6Rα was 11-fold increased in SV-T2 cells compared to BALB/c 3T3 cells, while that of gp130 was almost equivalent between the two cell lines (approximately 1.4-fold). Anti-IL-6Rα antibodies neutralized the IL-6-induced inhibition of proliferation in SV-T2 cells (Fig. 4). Thus we concluded that the inhibition was IL-6Rα-dependent. In this context, SV-T2 cells might acquire sensitivity to IL-6 via upregulated IL-6Rα.

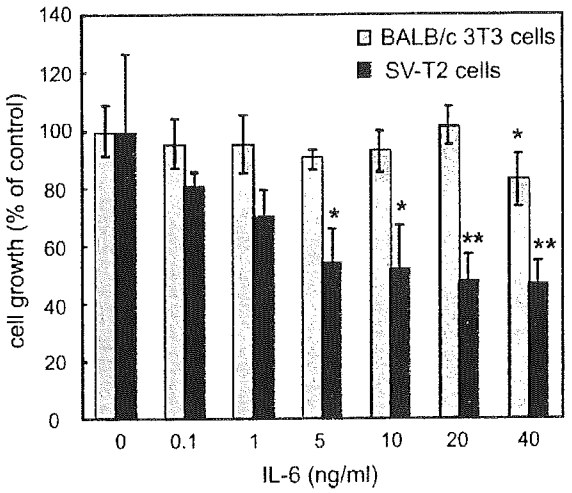

Fig. 3. Effect of IL-6 on the growth of BALB/c 3T3 and SV-T2 cells. Statistical significance, compared with that of IL-6 non-treated cells, is indicated by $*P < 0.05$ and $**P < 0.01$.

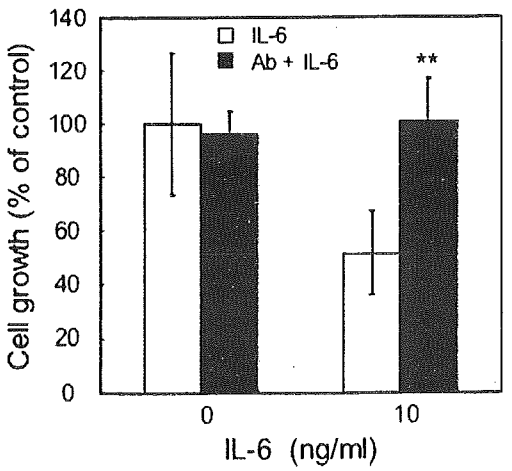

Fig. 4. Effect of anti-IL-6Rα antibodies on IL-6-treated SV-T2 cells. Cells were stimulated with 10 ng/ml of IL-6 in the presence, or absence, of anti-IL-6Rα and cultured for 5 days. Statistical significance, compared with that of IL-6 treated cells, is indicated by $**P < 0.01$.

Conclusion

The cell surface marker array developed on the DLC-coated glass slide has been successfully designed to carry the 378 oligo DNA probes for independent cell surface proteins. This microarray was employed here in profiling the gene expression of BALB/c 3T3 and SV-T2 cells. As a result, CD62L and IL-6Rα were found to be the candidates of the significantly upregulated genes in SV-T2 cells. RT-qPCR, immunohistochemical analysis and biological function analysis supported the result of microarray analysis. CD62L and IL-6Rα are proposed as the candidates of cell surface markers in SV-T2 cells. These data highlight the power of a DNA microarray with high reproducibility using the novel platform of a DLC-coated glass slide to identify cell surface markers, which might serve as molecular targets for the diagnosis or treatment of diseases. It is expected to expand the number of genes to cover all the cell surface markers for the arrays.

Acknowledgments

The authors thank Dr. Michifumi Tanga and Mr. Masayuki Kita for their continuous encouragement throughout the study. This study was supported by a Grant-in-Aid of the consortium for R&D projects for regional revitalization from METI.

References

[1] B.St. Croix, C. Rago, V. Velculescu, G. Traverso, K.E. Romans, E. Montgomery, A. Lal, G.J. Riggins, C. Lengauer, B. Vogelstein, K.W. Kinzler, Genes expressed in human tumor endothelium, Science 289 (2000) 1197–1202.

[2] W.J. Fairbrother, H.W. Christinger, A.G. Cochran, Novel peptides selected to bind vascular endothelial growth factor target the receptor-binding site, Biochemistry 37 (1998) 17754–17764.

[3] M.N. Fukuda, C. Ohyama, K. Lowitz, O. Matsuo, R. Pasqualini, E. Ruoslahti, M. Fukuda, A peptide mimic of E-selectin ligand inhibits sialyl Lewis X-dependent lung colonization of tumor cells, Cancer Res. 60 (2000) 450–456.

[4] J.H. Lee, J.A. Engler, J.F. Collawn, B.Az. Moore, Receptor mediated uptake of peptides that bind the human transferrin receptor, Eur. J. Biochem. 268 (2001) 2004–2012.

[5] H.B. Lowman, Y.M. Chen, N.J. Skelton, D.L. Mortensen, E.E. Tomlinson, M.D. Sadick, I.C. Robinson, R.G. Clark, Molecular mimics of insulin-like growth factor 1 (IGF-1) for inhibiting IGF-1: IGF-binding protein interactions, Biochemistry 37 (1998) 8870–8878.

[6] B.K. Kay, A.V. Kurakin, R. Hyde-Deruyscher, From peptides to drugs via phage display, Drug Discov. Today 3 (1998) 370–377.

[7] A.A. Alizadeh, D.T. Ross, C.M. Perou, M. van de Rijn, Towards a novel classification of human malignancies based on gene expression patterns, J. Pathol. 195 (2001) 41–52.

[8] J.M. Johnson, J. Castle, P. Garrett-Engele, Z. Kan, P.M. Loerch, C.D. Armour, R. Santos, E.E. Schadt, R. Stoughton, D.D. Shoemaker, Genome-wide survey of human alternative pre-mRNA splicing with exon junction microarrays, Science 302 (2003) 2141–2144.

[9] V. Syed, G. Ulinski, S.C. Mok, S.M. Ho, Reproductive hormone-induced, STAT3-mediated interleukin 6 action in normal and malignant human ovarian surface epithelial cells, J. Natl. Cancer Inst. 94 (2002) 617–629.

[10] T. Hirano, Interleukin 6 and its receptor: ten years later, Int. Rev. Immunol. 16 (1998) 249–284.

[11] K. Yamasaki, T. Taga, Y. Hirata, H. Yawata, Y. Kawanishi, B. Seed, T. Taniguchi, T. Hirano, T. Kishimoto, Cloning and expression of the human interleukin-6 (BSF-2/IFN beta 2) receptor, Science 241 (1988) 825–828.

0013-7227/05/$15.00/0
Printed in U.S.A.

Endocrinology 146(11):4673–4681

doi: 10.1210/en.2005-0456

Betacellulin-δ4, a Novel Differentiation Factor for Pancreatic β-Cells, Ameliorates Glucose Intolerance in Streptozotocin-Treated Rats

Takeki Ogata,†* Andrew J. Dunbar,* Yoritsuna Yamamoto, Yuji Tanaka, Masaharu Seno, and Itaru Kojima

Institute for Molecular and Cellular Regulation (T.O., Y.Y., I.K.), Gunma University, Maebashi 371-8512, Japan; Third Department of Medicine (T.O., Y.Y., Y.T.), National Defense Medical College, Tokorozawa 359-8513, Japan; GroPep Ltd. (A.J.D.), Adelaide SA 5000, Australia; and Department of Bioscience and Biotechnology (M.S.), Graduate School of Natural Science and Technology, Okayama University, Okayama 700-8530, Japan

We previously described a novel alternatively spliced mRNA transcript of the betacellulin (BTC) gene. This splice isoform, termed BTC-δ4, lacks the C-loop of the epidermal growth factor motif and the transmembrane domain as a result of exon 4 'skipping'. In this study, we expressed BTC-δ4 recombinantly to explore its biological function. When BTC-δ4 was expressed in COS-7 cells, it was secreted largely into the culture medium, in contrast to BTC. Unlike BTC, highly purified recombinant BTC-δ4 produced in *Escherichia coli* failed to bind or induce tyrosine phosphorylation of either ErbB1 or ErbB4, nor did it antagonize the binding of BTC to these receptors. Consistent with this, BTC-δ4 failed to stimulate DNA synthesis in Balb/c 3T3 and INS-1 cells. However, BTC-δ4 induced differentiation of pancreatic β-cells; BTC-δ4 converted AR42J cells to insulin-producing cells. When recombinant BTC-δ4 was administered to streptozotocin-treated neonatal rats, it reduced the plasma glucose concentration and improved glucose tolerance. Importantly, BTC-δ4 significantly increased the insulin content, the β-cell mass, and the numbers of islet-like cell clusters and PDX-1-positive ductal cells. Thus, BTC-δ4 is a secreted protein that stimulates differentiation of β-cells *in vitro* and *in vivo* in an apparent ErbB1- and ErbB4-independent manner. The mechanism by which BTC-δ4 exerts this action on β-cells remains to be defined but presumably involves an, as yet, unidentified unique receptor. (*Endocrinology* 146: 4673–4681, 2005)

MEMBERS OF THE epidermal growth factor (EGF) family are characterized by a high degree of sequence similarity, particularly with respect to a common six-cysteine 36- to 40-amino-acid residue EGF-motif with a spacing of $CX_7CX_{4-5}CX_{10-13}CX_1CX_8C$ that forms three intramolecular disulfide bonds (C_1-C_3, C_2-C_4, and C_5-C_6) and a characteristic three-loop structure (1). The EGF-motif of growth factor peptides belonging to this family all appear to be encoded by two exons with a precisely located intervening intron, corresponding to the border separating the first two disulfide loops (A loop, C_1-C_3; B loop, C_2-C_4) from the third loop (C loop, C_5-C_6) (2). A common feature of these molecules is that they are synthesized as larger transmembrane precursors that are proteolytically cleaved to release the soluble biologically active form of the growth factor. The consensus EGF-motif is crucial for binding to and activating members of the ErbB receptor tyrosine kinase family (1, 2). Four receptors belonging to this family have been identified (ErbB1/EGFR, ErbB2/HER2/Neu, ErbB3, and ErbB4). Ligand binding to ErbB receptors induces receptor homo- or heterodimerization, autophosphorylation, and subsequent activation of downstream signaling pathways, resulting in diverse physiological processes, including cell proliferation, differentiation, migration, and survival (3). Ligands belonging to this family include EGF; TGF-α; heparin-binding EGF; epiregulin; amphiregulin; the neuregulin subfamily, which includes the products of four genes (NRG1–4); and betacellulin (BTC). BTC binds and activates ErbB1 and ErbB4 homodimers and is further characterized by its ability to activate, albeit weakly, the highly oncogenic ErbB2/ErbB3 complex (4, 5). BTC was originally isolated as a growth factor synthesized in an insulinoma cell line (6). BTC is expressed abundantly in the intestine and pancreas (7). In the pancreas, BTC is expressed in non-β-cells of the islet in adults and is expressed in endocrine precursor cells in the fetus (8). This suggests the possibility that BTC regulates the growth and/or differentiation of pancreatic β-cells and their precursors. In accordance with this notion, BTC is able to induce differentiation of pancreatic AR42J cells and convert them into insulin-producing cells (9) and to convert glucagon-producing α-cells into β-cells (10). Furthermore, *in vivo* studies have shown that BTC promotes regeneration of pancreatic β-cells in various animal models of experimental diabetes (11–14). Collectively, BTC is a growth or differentiation factor for pancreatic β-cells.

We recently identified an alternately spliced mRNA tran-

First Published Online August 4, 2005

† This work is dedicated to the memory of Takeki Ogata, who sadly passed away during the completion of this manuscript.

* T.O. and A.J.D. contributed equally to this paper.

Abbreviations: BTC, Betacellulin; CM, culture medium; DAPI, 4′,6-diamidino-2-phenylindole; EGF, epidermal growth factor; HRP, horseradish peroxidase; ICC, islet-like cell cluster; ORF, open-reading frame; RP-HPLC, reverse-phase HPLC; TFA, trifluoroacetic acid; TUNEL, terminal deoxynucleotidyl transferase-mediated deoxyuridine 5-triphosphate nick end labeling.

Endocrinology is published monthly by The Endocrine Society (http://www.endo-society.org), the foremost professional society serving the endocrine community.

script encoding a novel isoform of human BTC (15). This isoform, originally termed BTC-β but now referred to as BTC-δ4, lacks 147 bp encoding exon 4 of the BTC gene, leading to the generation of an mRNA encoding an unusual BTC precursor in which the C-loop of the EGF domain and the transmembrane domain are deleted while the remainder of the mature molecule, including loops A and B and the 'hinge' valine, is fused in frame to the truncated C-terminal cytoplasmic tail (Fig. 1). Retention of the hydrophobic signal sequence and the absence of the transmembrane domain suggests that BTC-δ4 may be a secreted protein. Interestingly, a similar isoform lacking the third disulfide loop of the EGF domain has been reported for heparin-binding EGF (16). In this case, a 94-bp insertion between exons III and IV causes a frameshift and premature termination generating a protein that retains the signal peptide, proregion, heparin-binding domain and the first two conserved disuphide loops of the EGF motif, while a short nine-amino-acid tail replaces the third disulfide loop, transmembrane, and cytoplasmic domains. In this report, we have produced BTC-δ4 recombinantly to characterize it's biological activity and, in particular, to determine whether it may act as a naturally occurring BTC antagonist. Our results indicate that whereas BTC-δ4 does not bind to either ErbB1, ErbB4, or the ErbB2–3 heterodimeric complex and shows no evidence of acting as an BTC antagonist, BTC-δ4 is biologically active and acts as an inducer of differentiation of pancreatic β-cells *in vitro* and *in vivo*, possibly through a novel cell surface receptor.

Materials and Methods

Reagents

Recombinant human activin A was a generous gift from Dr. Y. Eto of Central Research Laboratory, Ajinomoto Inc. (Kawasaki, Japan). Streptozotocin (STZ) was purchased from Wako Pure Chemicals (Osaka, Japan). Mouse fibroblast Balb/c 3T3 cells were from the American Type Culture Collection (Manassas, VA). Human lung fibroblast AG2804 cells and CHO cells transfected with either ErbB 4 or ErbB2/3 were kindly provided by Dr. J. Gunn (Texas A&M University, College Station, TX) and Prof. Y. Yarden (Weizmann Institute, Rehovet, Israel), respectively. INS-1 cells were generously provided by Prof. C. Wollheim (University of Geneva, Geneva, Switzerland). Anti-FLAG M2 antibody was from Sigma (St. Louis, MO). Anti-ErbB1 (1005), anti-ErbB4 (C-18), and antiphosphotyrosine (PY20) antibodies were from Santa Cruz Biotechnology, Inc. (Santa Cruz, CA) and horseradish peroxidase (HRP)-conjugated rabbit antisheep antibody from Zymed Laboratories (San Francisco, CA). HRP-conjugated sheep antimouse antibody was from Silenus Laboratories (Hawthorn, Australia). Lipofectamine 2000, Enterokinase, *Escherichia coli* TOP10 cells, Optimem-1, 10–20% Tris Tricine gels, and pcDNA3.1 were from Invitrogen (Carlsbad, CA). West Pico SuperSignal substrate was from Pierce Biotechnology, Inc. (Rockford, IL) pET32, BL21*trxB* (DE3) cells, and BugBuster Protein Extraction Reagent were from Novagen; Ni-NTA agarose was from QIAGEN (Valencia, CA). Recombinant human BTC and goat antihuman BTC ectodomain (Asp_{32}-Tyr_{111}) antibody were from R&D Systems, Inc. (Minneapolis, MN). Complete protease inhibitors and protein G-Sepharose were from Roche Molecular Biochemicals (Basel, Switzerland).

Cloning of BTC and BTC-δ4 FLAG-tagged constructs

Full-length BTC (amino acids Met_1-Ala_{178}) and BTC-δ4 (amino acids Met_1-Ala_{120}) were cloned into pcDNA3.1 to generate expression vectors for the mammalian production of BTC and BTC-δ4 as follows. The open-reading frames (ORFs) of BTC and BTC-δ4 were excised from pBlue-BTC-δ4 and pBlue-BTC (15) with *Apa*I and *Bam*HI and recloned into *Apa*I/*Bam*HI digested pcDNA3.1. To generate 'Flag-tagged' pcDNA3.1-BTC-δ4 and pcDNA3.1-BTC constructs, in which the Flag epitope DYKDDDDK is inserted between amino acids S35–T36, pcDNA3.1-BTC-δ4 or pcDNA3.1-BTC was used as a template in PCR using the primers; 5′-CTCGGGAATTCCGACTACAAGGACGACGATGACAAGACCAGAAGTCCTGAA-3′ (sense) (*underlined* nucleotides correspond to an *Eco*RI restriction site; *double underlined* nucleotides encode the FLAG epitope tag) and 5′-CTCCTGCAGTTAAGCAATATTTGTCTCTTC-3′ (antisense) (*underlined* nucleotides correspond to a *Pst*I restriction site). The resulting PCR products were purified and digested with *Eco*RI and *Pst*I and cloned into *Eco*RI/*Pst*I digested pBlue-BTC or pBlue-BTC-δ4. Subsequently, the resultant Flag-tagged pBlue-BTC and pBlue-BTC-δ4 constructs were digested with *Apa*I/*Bam*H1 and cloned into *Apa*I/*Bam*H1 digested pcDNA3.1 to generate pcDNA3.1-FLAG-BTC-δ4 and pcDNA3.1-FLAG-BTC.

Expression and analysis of BTC and BTC-δ4 FLAG-tagged constructs in COS-7 cells

For transient expression of pcDNA3.1-FLAG-BTC-δ4 and pcDNA3.1-FLAG-BTC, COS-7 cells were plated into 12-well plates, at 2×10^5 cells/well, in DMEM/10% fetal bovine serum. After overnight incubation, cells were transfected with 2 μg construct DNA using Lipofectamine 2000 and Optimem-1 media according to the manufacturer's instructions. Twelve hours later, the cells were washed twice and replenished with fresh Optimem-1 media. Seventy-two hours post transfection, culture medium (CM) was collected and cell lysates prepared. CM was clarified by centrifugation, and the presence of BTC or BTC-δ4 in the media was analyzed by ELISA or Western blotting using an anti-FLAG-M2 antibody (Sigma). BTC or BTC-δ4 present in the cell lysate was analyzed by Western blotting with the anti-FLAG-M2 antibody. Cell lysates were prepared by washing the cells twice with PBS after the removal of CM and then lysing the cells directly in SDS-PAGE sample buffer and heating to 95 C for 5 min. For ELISA analysis of the CM, 90 μl of CM was mixed with 10 μl of 10× coating buffer (0.15 mol/liter Na_2CO_3, 0.35 mol/liter $NaHCO_3$, pH 9.3) and loaded into 96-well immunosorbent plates. Plates were coated overnight at 4 C, then blocked in 2% BSA in PBS/0.1% Tween (PBS-T). Plates were washed four times with PBS-T and then incubated for 1 h at 37 C with anti-FLAG antibody diluted in PBS-T (2.5 μg/ml). After incubation, plates were washed as above and incubated with HRP-conjugated sheep antimouse antibody (1:2000) diluted in PBS-T. Plates were then washed four times with PBS-T and developed with *o*-phenylamine diamine substrate and stopped with 2 mol/liter H_2SO_4. Absorbance was read at 490 nm. Results are expressed as the mean ± SD of triplicate determinations. To analyze

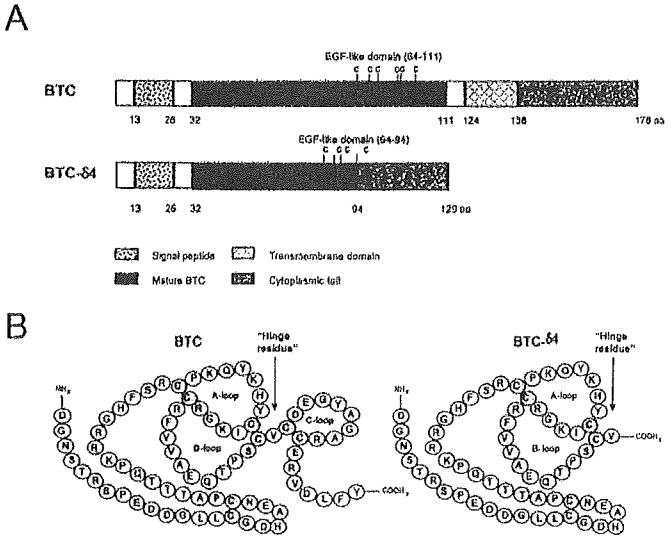

FIG. 1. Schematic representation of the domain structure of the BTC and BTC-δ4 isoforms. A, The relationship between BTC and BTC-δ4 primary translation products. B, Secondary structure relationship of the EGF-motif for BTC and BTC-δ4. For simplicity, the cytoplasmic domain of BTC-δ4 (Pro_{95}-Ala_{120}), which is fused in-frame to the hinge Val94 residue is not shown.

the presence of BTC or BTC-δ4 on the cell surface by ELISA, CM was removed and the cells washed three times with PBS. The cells were then fixed with 4% paraformaldehyde and stained with anti-FLAG M2 antibody as described above. For Western blot analysis with the anti-FLAG-M2 antibody, CM or cell lysates were resolved by SDS-PAGE (10–20% Tris-Tricine gels). Proteins were then transferred to nitrocellulose (Hybond-C extra; Amersham Pharmacia Biotech, Little Chalfont, UK) and membranes probed with mouse anti-FLAG-M2 antibody (2.5 μg/ml) and then HRP-conjugated sheep antimouse antibody (1:10,000). HRP-labeled proteins were visualized using SuperSignal West Dura Extended Duration Substrate.

Expression and purification of BTC and BTC-δ4

BTC-δ4 [constituting amino acids Asp_{32}-Ala_{129} (BTC-$δ4_{32-129}$)] (Fig. 1) was expressed as a thioredoxin fusion protein in pET32a. The ORF sequence of BTC-$δ4_{32-129}$ was amplified by PCR using the primer set, 5′-CGTCCATGGCTGATGGGAATTCCACCAGAAGT-3′ (sense) and 5′-CGTCTCGAGTCATTAAGCAATATTTGTCTCTTC-3′ and pBlue-BTC-δ4 (15) as template. *Nco*I and *Xho*I recognition sites were attached to the sense and antisense primers, respectively (*underlined*). BTC (constituting amino acids 32–111; BTC_{32-111}) was also expressed using the pET system as a positive control, as described previously (7), or produced as a thioredoxin fusion protein with the plasmid pET32a. For this construct, the ORF sequence of BTC_{32-111} was amplified by PCR using the primer set, 5′-CGTCCATGGCTGATGGGAATTCCACCAGAAGT-3′ (sense) and 5′-CGTCTCGAGTCAGTAAAACAAGTCAACTGT-3′ (antisense) and pBlue-BTC (see Ref. 18) as template. *Nco*I and *Xho*I recognition sites were also attached to the sense and antisense primers, respectively (*underlined*). The PCR products were digested with *NcoI*/*XhoI* and cloned into *NcoI*/*XhoI* digested pET32a vector as above. The resultant plasmids, pETBTC-$δ4_{32-129}$ and pETBTC_{32-111}, were maintained in *Escherichia coli* JM109 and, for expression, transformed into *Escherichia coli* BL21*trxB* (DE3) cells. Large-scale expression of BTC or BTC-δ4 in BL21*trxB* (DE3) cells was carried out as described in the pET system manual (Novagen, Madison, WI). BTC or BTC-δ4 thioredoxin fusion proteins were purified from clarified cell lysates by Ni-NTA agarose affinity, followed by cleavage with Enterokinase to isolate authentic BTC or BTC-δ4. Authentic BTC or BTC-δ4 was separated from the thioredoxin fusion partner by additional Ni-NTA agarose affinity chromatography and reverse-phase HPLC (RP-HPLC). Briefly, frozen cell pellets were thawed on ice and resuspended in 18 ml BugBuster Protein Extraction Reagent containing lysozyme (100 μg/ml) and incubated at room temperature with gentle shaking for 10 min. After incubation, the cell lysate was sonicated (3 × 5-sec bursts) and clarified by centrifugation (20 min, 16,000 rpm, 10 min). The clarified cell lysate was adjusted to 10 mmol/liter imidazole and applied to a Ni-NTA agarose affinity column preequilibrated with 50 mmol/liter NaH_2PO_4, 0.3 mol/liter NaCl, 10 mmol/liter imidazole (pH 8.0). After column washing with 50 mmol/liter NaH_2PO_4, 0.3 mol/liter NaCl, 40 mmol/liter imidazole (pH 8.0), BTC or BTC-δ4 was eluted with 50 mmol/liter NaH_2PO_4, 0.3 mol/liter NaCl, 250 mmol/liter imidazole (pH 8.0) and subsequently dialyzed overnight (Spectra/Por, 3.5 kDa MWCO; Spectrum Laboratories, Houston, TX) against several changes of Enterokinase cleavage buffer (50 mmol/liter Tris-Cl, 1 mmol/liter CaCl2, 0.1% Tween 20, pH 7.4). To remove the thioredoxin fusion partner from BTC or BTC-δ4, Enterokinase was added to a final concentration of 0.1 U/20 μg protein and incubated overnight at 37 C with gentle mixing. BTC or BTC-δ4 was separated from the thioredoxin fusion partner by further Ni-NTA agarose affinity chromatography as described above. In this case, the cleaved thioredoxin fusion partner is captured on the resin and BTC or BTC-δ4 is collected in the flow-through fraction flow-through fraction. BTC or BTC-δ4 present in the flow-through fraction was further purified by RP-HPLC. Briefly, the Ni-NTA agarose flow-through fraction was diluted 1:4 (vol/vol) with 0.1% trifluoroacetic acid (TFA) and applied to a C4 Prep-Pak RP-HPLC column (25 mm × 100 mm; 300, 15 μm; Millipore-Waters, Bedford, MA) at a flow rate of 10 ml/min. The column was washed with 0.1% TFA and eluted with a gradient of 8–80% (vol/vol) acetonitrile over 150 min in the presence of 0.08% TFA at a flow rate of 10 ml/min. Twenty-milliliter fractions were collected, and aliquots of each (50 μl) were analyzed by SDS-PAGE and Western blotting using a goat antihuman BTC ectodomain (Asp_{32}-Tyr_{111}) antibody to identify pure BTC or BTC-δ4 containing fractions. The purity of all BTC or BTC-δ4 preparations were analyzed by analytical RP-HPLC, electrospray ionization mass spectrometry, and SDS-PAGE. Analytical RP-HPLC was performed using a Brownlee aquopore C4 RP-HPLC column (2.1 × 100 mm) (Alltech, Deerfield, IL) with a linear gradient of 8–80% (vol/vol) acetonitrile and 0.08% TFA over 40 min at a flow rate of 0.5 ml/min. Alternatively, BTC-$δ4_{32-129}$ (containing an initiation methionine residue) was cloned into the expression vector pET3b to construct pBO604, and the recombinant protein was solubilized and refolded from inclusion bodies, purified through cation exchange column and gel filtration column chromatography as previously described (7, 17). The authenticity of BTC-$δ4_{32-129}$ was confirmed by amino-terminal sequence analysis and amino acid composition. All the recombinant proteins prepared in this study were lyophilized and stored at −80 C before use.

ErbB-receptor binding and mitogenic activity of BTC-δ4

The binding affinity of BTC or BTC-δ4 to ErbB receptors was determined by measuring the ability of BTC or BTC-δ4 to competitively displace [^{125}I]-labeled recombinant human BTC from ErbB1 or ErbB4 receptors present on AG2804 fibroblasts or CHO cells stably transfected with ErbB4 (18) as described previously (19). The mitogenic activity of BTC and BTC-δ4 toward Balb/c 3T3 fibroblasts and INS-1 cells was performed as previously described (19).

Analysis of ErbB-1 and ErbB-4 receptor tyrosine phosphorylation

AG2804 or CHO-ErbB4 cells were grown to confluence in 10-cm dishes and subsequently incubated for 12–14 h in serum-free medium. Cells were then stimulated with 10 nmol/liter BTC, BTC-δ4, or a combination of both for 10 min at room temperature. After stimulation, cells were washed twice in PBS and then lysed in lysis buffer (0.5 ml) (50 mmol/liter Tris-Cl, pH 7.4; 150 mmol/liter NaCl; 1% deoxycholate; 1% Triton X-100; 0.1% sodium dodecyl sulfate; 5 mmol/liter sodium orthovanadate; 10 mmol/liter sodium fluoride; 1 mmol/liter EGTA; and complete protease inhibitors. Cell lysates were cleared by centrifugation (20 min, 15,000 × *g* at 4 C) and ErbB1 or ErbB4 immunoprecipitated by incubating the lysate with 1 μg rabbit polyclonal anti-ErbB1 antibody (1005, Santa Cruz) or rabbit polyclonal anti-ErbB4 antibody, respectively, for 2 h at 4 C with gentle shaking. After incubation, protein-G Sepharose was added and the mixture incubated for a further 1 h at 4 C. Immune complexes were collected by centrifugation, washed three times in lysis buffer, and heated (3 min, 95 C) in SDS-PAGE sample buffer. Proteins were separated by SDS-PAGE (10–20% Tricine gels) and transferred to nitrocellulose filters (Hybond C; Amersham). Membranes were probed with antiphosphotyrosine monoclonal antibody (PY20) and then with HRP-conjugated sheep antimouse antibody. HRP-labeled proteins were visualized using enzyme-linked chemiluminescence (Amersham). To confirm equal loading, blots were stripped and reprobed with rabbit polyclonal anti-ErbB1 or rabbit polyclonal anti-ErbB4 antibodies and HRP-conjugated rabbit antisheep antibody.

Measurement of differentiation and apoptosis of AR42J cells

AR42J-B20 cells were cultured in DMEM medium containing 10% fetal calf serum as described previously (9). To assess differentiation into insulin-producing cells, cells were incubated for 48 h with 2 nmol/liter activin A and either 1 nmol/liter BTC or BTC-δ4. Cells were then fixed and stained with antiinsulin or anti-C peptide antibody as described previously (9, 20), and the number of insulin-positive cells was counted. Nuclei were stained with 4′,6-diamidino-2-phenylindole (DAPI). Apoptosis was assessed by using a terminal deoxynucleotidyl transferase-mediated deoxyuridine 5-triphosphate nick end labeling (TUNEL) technique (Wako Pure Chemicals.). Changes in the number of viable cells were assessed by using 3-[4,5-dimethylthiazole-2-yl]-2,5,-dipheltetrazodium bromide (MTT) (21). Anti-C-peptide antibody was obtained from Linco Research, Inc. (St. Charles, MS).

Treatment of neonatal rats with streptozotocin

One-day-old Sprague Dawley rats were treated with streptozotocin and tested for blood glucose levels as described previously (14). The

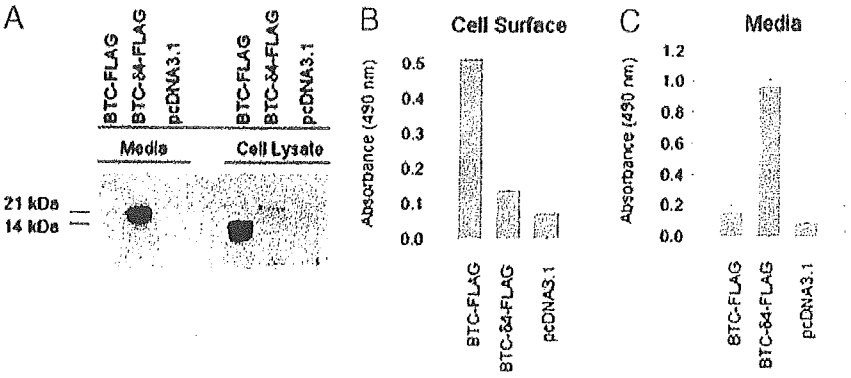

FIG. 2. BTC-δ4 is a secreted protein. A, COS-7 cells were transiently transfected with either BTC-FLAG, BTC-δ4-FLAG, or empty vector (pcDNA3.1). Seventy-two hours post transfection, the CM was collected and cell lysates prepared. CM and cell lysates were analyzed by Western blot with an anti-FLAG M2 antibody. B, COS-7 cells were transfected as above and CM or nonpermeabilized fixed cells analyzed by ELISA with anti-FLAG M2 antibody. Note, similar results for Western blot and ELISA were also obtained with an anti-BTC ectodomain antibody (R&D Systems) (data not shown).

animals were included in the study only if the blood glucose concentration was between 200 and 350 mg/dl on the next day (designated as d 0). Animals whose blood glucose was more than 350 mg/dl on d 0 developed severe diabetes, and the blood glucose concentrations in these animals were more than 600 mg/dl on d 1 or 2. Neonatal STZ-treated rats were injected with 3 pmol/g BTC-δ4, BTC, or saline every day for 5 d starting from d 0. The fasting blood glucose concentration and the body weight were measured daily for the first week and then once a week for up to 8 wk. Two months after the STZ treatment, an ip glucose tolerance test (2 g/kg body weight) was performed after 14 h of fasting. The experimental protocol was approved by the Animal Care Committee of the Gunma University.

Tissue processing and immunohistochemistry

On d 4 and wk 8, the animals were injected ip with 1 ml bromodeoxyuridine labeling reagent per 100 g body weight (cell proliferation kit; Amersham) and decapitated after 3 h. The pancreas was excised, weighed, and divided into two parts. One portion from the splenic segment was fixed with 4% paraformaldehyde/PBS overnight at 4 C and processed for paraffin embedding. Four series from each pancreas were cut, at intervals of 100 μm in neonates and 300 μm in adults, for immunostaining and histochemistry. The second portion was homogenized in cold acid-ethanol, heated for 5 min in 70 C water bath, and centrifuged, and the supernatant was stored at −20 C before assaying for insulin. Insulin was measured by time-resolved immunofluorometric assay as described previously (9). Immunohistochemistry was performed as described previously (12, 13). Quantitation of the β-cell mass was performed on insulin-stained sections using image analysis software (National Institutes of Health image) by means of an AX70 Epifluorescence microscope (Olympus Corp., Tokyo, Japan) equipped with a PXL 1400 cooled-charge-coupled device camera system (Photometrics, Tucson, AZ) operated with IP Lab Spectrum software (Signal Analysis, Vienna, VA). At least 40 random fields (magnification, ×200) from one section (three sections from different series per block) were measured for the area of insulin-positive cells. The β-cell mass was calculated as described elsewhere (12, 13). To quantify β-cell neogenesis, the number of islet-like cell clusters (ICCs) (less than five cells across) was determined. The number of ICCs and islets was counted in the section stained with the antiinsulin antibody, and the area in these sections was measured. At least five sections were analyzed per animal. Results were expressed as means ± SE. For comparisons between two groups, the unpaired *t* test was used.

Results

BTC-δ4 is a secreted protein

Like other members of the EGF family, BTC is synthesized as a transmembrane-anchored precursor protein (pro-BTC), which can be proteolytically cleaved to yield soluble BTC containing the EGF-motif (Asp_{32}-Tyr_{111}). Retention of the hydrophobic signal peptide and the absence of the transmembrane domain suggest that BTC-δ4 may be a secreted protein. To test this, the complete ORF of either BTC or BTC-δ4 (additionally engineered to incorporate a FLAG epitope between amino acids Ser35 and Thr36 for subsequent detection) was cloned into the expression vector pcDNA3.1 and secretion monitored after transient transfection in COS-7 cells. Seventy-two hours post transfection, BTC-δ4-FLAG was clearly detected in the culture supernatant by either Western-blot (~14 kDa) or enzyme immunoassay, with very little present in the cell lysate or on the cell surface (Fig. 2, A and B). In contrast, BTC-FLAG was predominantly present

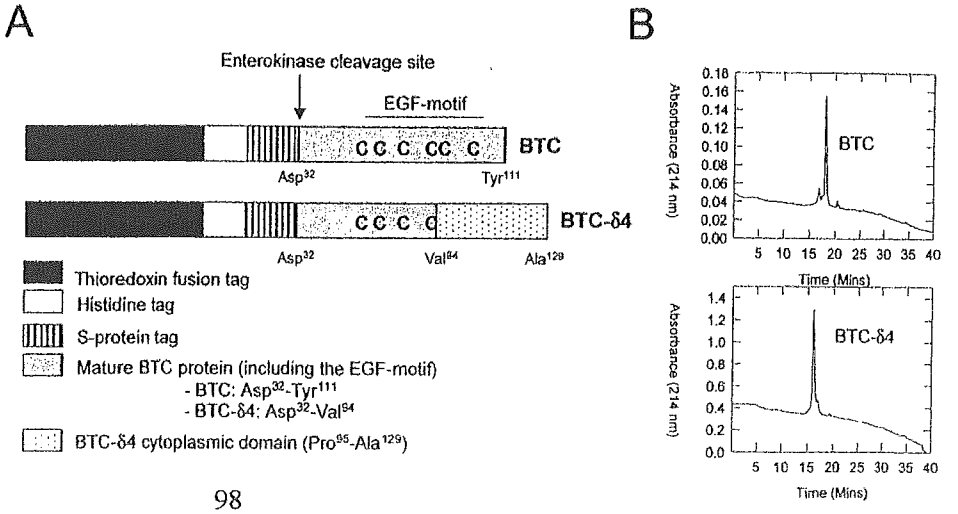

FIG. 3. Recombinant expression and purification of BTC and BTC-δ4. A, The mature form of BTC (Asp_{32}-Tyr_{111}) or full-length BTC-δ4 (Asp_{32}-Ala_{129}, minus the hydrophobic signal peptide Met_1-Ala_{31}) were expressed as thioredoxin fusion proteins in the bacterial expression vector pET3.2a, pET3.2a-BTC and pET3.2a-BTC-δ4 constructs were transformed into the *Escherichia coli* strain BL21(*DE3*) and proteins expressed after induction with isopropyl β-D-thiogalactoside. After induction, cells were collected and lysed and BTC or BTC-δ4 purified by Ni-NTA agarose and RP-HPLC. B, The purity of each BTC or BTC-δ4 preparation was assessed by analytical C4 RP-HPLC.